



A critical review on direct catalytic hydrogasification of coal into CH₄: catalysis process configurations, evaluations, and prospects

Shuai Yan^{1,2} · Jun Feng³ · Shenfu Yuan⁴ · Zihong Xia⁵ · Fengshuang Han^{1,2} · Xuan Qu³ · Jicheng Bi³

Received: 15 June 2023 / Revised: 24 October 2023 / Accepted: 5 March 2024
© The Author(s) 2024

Abstract

Coal catalytic hydrogasification (CCHG) is a straightforward approach for producing CH₄, which shows advantages over the mature coal-to-CH₄ technologies from the perspectives of CH₄ yield, thermal efficiency, and CO₂ emission. The core of CCHG is to make carbon in coal convert into CH₄ efficiently with a catalyst. In the past decades, intensive research has been devoted to catalytic hydrogasification of model carbon (pitch coke, activated carbon, coal char). However, the chemical process of CCHG is still not well understood because the coal structure is more complicated, and CCHG is a combination of coal catalytic hydrothermal gasification and coal char catalytic hydrogasification. This review seeks to shed light on the catalytic process of raw coal during CCHG. The configuration of suitable catalysts, operating conditions, and feedstocks for tailoring CH₄ formation were identified, and the underlying mechanisms were elucidated. Based on these results, the CCHG process was evaluated, emphasizing pollutant emissions, energy efficiency, and reactor design. Furthermore, the opportunities and strategic approaches for CCHG under the restraint of carbon neutrality were highlighted by considering the penetration of “green” H₂, biomass, and CO₂ into CCHG. Preliminary investigations from our laboratories demonstrated that the integrated CCHG and biomass/CO₂ hydrogenation process could perform as an emerging pathway for boosting CH₄ production by consuming fewer fossil fuels, fulfilling the context of green manufacturing. This work not only provides systematic knowledge of CCHG but also helps to guide the efficient hydrogenation of other carbonaceous resources such as biomass, CO₂, and coal-derived wastes.

Keywords Coal gasification · Catalytic hydrogasification · Methane · Pressurized fluidized bed

✉ Xuan Qu
quxuan123@sxicc.ac.cn

¹ School of Materials and Chemical Engineering, Ningbo University of Technology, Ningbo 315211, Zhejiang, China

² Zhejiang Institute of Tianjin University, Ningbo 315201, Zhejiang, China

³ State Key Laboratory of Coal Conversion, Institute of Coal Chemistry, Chinese Academy of Sciences, Taiyuan 030001, China

⁴ School of Chemical Science and Engineering, Key Laboratory of Medicinal Chemistry for Natural Resource, Ministry of Education, National Center for Experimental Chemistry and Chemical Engineering Education Demonstration, Yunnan Provincial Key Laboratory of Carbon Neutral and Green Low-Carbon Technology, Yunnan University, Kunming 650091, China

⁵ Department of Energy and Chemical Engineering, East China University of Science and Technology, Shanghai 200237, China

List of symbols

AAEMs	Alkali–alkaline earth metals
Ar	Archimedes constant
BTX	Benzene, toluene, and xylenes
C2–C3	C ₂ H ₆ , C ₂ H ₄ , C ₃ H ₈ , and C ₃ H ₆
Cat-DH	Catalytic depolymerization and hydrogenation
Cat-HC	Catalytic hydrocracking
CCHG	Coal catalytic hydrogasification
CCG	Coal catalytic gasification
CHG	Coal hydrogasification
Co–Ca	Cobalt–calcium binary catalyst
co-CCHG	Combining coal catalytic hydrogasification and biomass hydrogasification
CS	Corn stalks
D	Inner diameter of fluidized bed (m)
DFT	Density functional theory
d _p	Coal particle diameter (m)
FG	Fugu bituminous coal
H	Height of dense phase bed (m)
HCL	Hydrocarbon liquids

LHV	Lower heating value
N	Fluidization number
P^0	Standard pressure (Pa)
P_{CH_4}	CH_4 partial pressure (Pa)
PCX	Phenol, cresols, and xylenols
P_{H_2}	H_2 partial pressure (Pa)
PRT	Particle residence time
PS	Particle size
r	H_2/coal mass ratio
R	Universal gas constant (J/mol K)
Re	Reynolds number
Re_{mf}	Reynolds number at the minimum fluidization velocity
RE	Renewable energy
RTZ	Reaction zone temperature
SHM	Shanghaimiao high sulfur sub-bituminous coal
SNG	Substituted natural gas
STP	Standard temperature and pressure
T	Temperature (K)
t	Residence time of coal particle (h)
TEM	Transmission electron microscopy
TSG	Two-stage gasification
J	Reaction quotient
u	Gas velocity (m/s)
u_{mf}	Minimum fluidization velocity (m/s)
V_{CH_4}	CH_4 formation rate (mL/g min)
VM	Volatile matter
W	Mass feeding rate of coal (kg/h)
XRD	X-ray diffraction
Y_{CH_4}	CH_4 yield (%)
YM	Yimin lignite
YQ	Yangquan anthracite
ZJX	Zhujixi bituminous coal
ΔG^\ominus	Standard Gibbs free energy change (J/mol)
ΔG	Gibbs free energy change at certain reaction conditions (J/mol)
ΔH	Reaction heat (kcal/mol)
ρ_{g}	H_2 density (kg/m^3)
ρ_{p}	Coal particle density (kg/m^3)
μ_{g}	H_2 viscosity (Pa s)
E_{mf}	Bed voidage at the minimum fluidization velocity

1 Introduction

Substituted natural gas (SNG), an important low-carbon and clean fuel, is characterized by a limited reserve compared to coal in Asian and European Union countries (Si et al. 2022). It is predicted that the SNG consumption in these countries will continuously increase, while more than 40% of them rely on importation (Xie 2021). For the security of

energy structure, there is a great necessity for developing the technology of coal-to-SNG. Especially in recent years, the requirement for reducing greenhouse gas emissions motivates the low-carbon utilization of coal.

The coal-to-SNG technologies are often categorized into two-stage gasification (TSG), coal catalytic gasification (CCG), and coal hydrogasification (CHG) (Suuberg et al. 1980; He et al. 2013; Yuan et al. 2018; Chang et al. 2020). The TSG represented by the Lurgi gasifier has been commercialized, while the CCG and CHG are under demonstration (Li et al. 2021). TSG produces CH_4 through various units, including coal gasification, water–gas shift reaction, and methanation. A long process characteristics TSG, and the endothermic and exothermic reactions are conducted separately, resulting in low thermal efficiency (61.9%) and high investment (Yuan 2020). CCG integrates the endothermic and exothermic reactions in one reactor with the aid of potassium/sodium catalysts, and thus, the energy efficiency is improved (71.4%) (Steinberg 2005). However, the methanation process in CCG is thermodynamically limited because all of the reactions in CCG take place at a relatively high temperature (~ 700 °C) (Hirsch et al. 1982). Therefore, CCG is characterized by high coal conversion ($\sim 95\%$) and low CH_4 yield ($\sim 25\%$). From the perspective of CH_4 production, CHG is the most appealing route, as it produces CH_4 with a high yield (30%–50%) and thermal efficiency (79.6%) (Steinberg 2005; Yuan et al. 2018). However, the essence of CHG is a hydrolysis process. Suffering from the low C– H_2 reactivity, a large amount of inert carbon remains unconverted, although harsh reaction conditions (850–1100 °C, 5–7 MPa) are adopted (Mısırlıoğlu et al. 2007). A large amount of char residue needs to be reused, which results in a high post-processing load and a low handling capacity.

Catalytic hydrogasification is an effective approach to accelerate the conversion of inert carbon under mild conditions (750–850 °C, 1–3 MPa) (Tomita and Tamai 1972; Haga and Nishiyama 1987; Qu et al. 2022). Since the 1980s, many research institutions have performed laboratory-scale investigations of catalytic hydrogasification with model carbon (graphite, activated carbon, pitch coke, and coal char) as the raw materials, and the alkali and transition metals were proved as the suitable catalysts (Casanova et al. 1983; Nishiyama 1986; Zoheidi and Miller 1987; Matsumoto et al. 1991). It is well accepted that catalytic hydrogasification of model carbon follows two crucial steps: supplying active hydrogen ($\text{H}\cdot$) and activating C=C bonds (Tamai et al. 1977; Haga and Nishiyama 1983; Han et al. 2022). The catalysts mainly participate in these two processes to accelerate the C– H_2 reaction. It is also well recognized that the reactivity of catalytic hydrogasification is determined by many factors, such as the nature of catalysts, including addition amount, dispersion, and component, and the properties of model

carbon consist of surface area, ash/sulfur content, and degree of condensation (Tomita et al. 1983; Liu et al. 2017a, 2017b; Zhang et al. 2019; Saraceno et al. 2023). Disappointingly, although great progress had been made in catalytic hydrogasification of model carbon, the trail nearly ceased and did not extend to catalytic hydrogasification of coal because of the low economic attractiveness of SNG in the 1980–2000s. As a result, plenty of fundamental issues remain unsolved, such as the best configuration of catalyst, the crucial step for C–H₂ catalytic reaction, the behavior of catalyst in catalytic hydrogasification of coal, et al. A clear elaboration of the above issues is worthwhile because it is not only helpful for the design of catalyst and feedstocks, but also provide strategies for regulating reaction process to tailor the generation of target products.

In the practical production process, raw coal instead of model carbon prefers to be used as the raw material. Compared to that of model carbon catalytic hydrogasification, coal catalytic hydrogasification (CCHG) has the following merits (Anthony and Howard 1976; Yan et al. 2017; Yuan et al. 2018): (1) Coal resource is abundantly distributed and ready for use; (2) Raw coal has less ordered carbon structure than that of the model carbon, which possesses relatively high reactivity itself; (3) CCHG produces additional high value-added HCL (hydrocarbon liquids) including ‘benzene, toluene, xylenes’ (BTX), ‘phenol, cresols, xylenols’ (PCX) and naphthalene. However, raw coal is a complex heterogeneous material with various chemical and physical properties, and catalysis in coal hydrogasification is significantly affected by coal properties (Yuan et al. 2015). In addition, the catalyst not only catalyzes hydrogasification of coal char, but also affects the hydrolysis of raw coal, which in turn shows enormous effects on coal char hydrogasification (Yan et al. 2018), making the CCHG process complicated. To

date, most of the studies mainly concentrated on catalytic hydrogasification of model carbon, while the detailed catalysis process of coal hydrogasification remains ambiguous.

The interest in CCHG was stimulated in the past decade due to the rapid growth in price and demand for SNG. In addition, the endowment that CCHG produces CH₄ and HCL simultaneously with high yield and high thermal efficiency (Table 1) under a mild reaction condition also contributes to the widespread attention (Gao et al. 2020; Yan et al. 2022). Efforts have been made to explore effective catalysts, proper reaction conditions, and catalytic mechanisms (Takarada et al. 1997; Qu et al. 2019; Sun et al. 2019). There appears to be a consensus that the recoverability of catalysts, the feedstock adaptability, and the availability of low-cost hydrogen are the crucial factors affecting the commercialization of CCHG. Fortunately, the first two issues have been preliminarily addressed in recent years (Yan et al. 2017, 2021), which will be discussed in Sects. 3 and 4. In terms of H₂, it can be produced from coal-based syngas, coke oven gas, chlorine alkali plants, or renewable energy (RE) based gasification or electrolysis (Saeidi et al. 2021). The last route has been proposed as a competitive H₂ generation approach in the next ten years (Ipsakis et al. 2021), which can realize the insertion of RE into chemical and fuel production processes used in modern societies. Moreover, integrating RE-based H₂ and CCHG is feasible to resolve the challenging H₂ storage and transport process. Meanwhile, the existing infrastructure stores and transports SNG products easily, and the integrated process offers high flexibility to stabilize electricity grids with a high share of renewable resources, thus enabling long-term low-carbon running. Notably, China’s commitments to the international community regarding carbon peak and neutral targets set higher requirements for coal utilization. As CCHG has the potential

Table 1 Comparison of the coal-to-SNG technologies

Process	Lurgi (Chen et al. 2017)	CCG (Hirsch et al. 1982; Yuan et al. 2017a, b)	CHG (Anthony and Howard 1976; Steinberg et al. 2005)	CCHG (Yan et al. 2017)
Reactor	Fixed bed	Fluidized bed	Entrained-flow bed	Fluidized bed
Catalyst	No	K ₂ CO ₃	No	Co and Ca nitrate
Particle	Lump coal	Powder coal	Powder coal	Powder coal
Gasifying agent	H ₂ O	H ₂ O	H ₂	H ₂
Temperature (°C)	900–1000	700	900–1100	850
Pressure (MPa)	2.0–4.0	3.5	5.0–7.0	3.0
Residence time	1–3 h	2 h	15–20 s	0.5 h
Carbon conversion	~99%	~95%	~50%	90%
CH ₄ yield	~20.3%	~33.3%	~35.0%	77.3%
CH ₄ production (Nm ³ /kg coal)	0.32	0.52	0.55	1.11
CO ₂ emission (g/mol CH ₄)	72.64	44.84	36	38.25
Catalyst recovery	–	~87.6%	–	>99%
Thermal efficiency	61.9%	72.7%	79.6%	81.8%

to convert coal in a clean, efficient, and low-carbon manner, it is therefore proposed as an alternative technology for the traditional TSG and CCG in SNG production.

There have been many excellent reviews on converting coal to methane in the past through the approach of TSG, CCG, and CHG. (Hirsch et al. 1982; Li et al. 2021) summarized the technologies of CCG and TSG comprehensively. In these processes, H_2O acts as the gasifying medium, and coal reacts with H_2O to form CH_4 with alkali/alkaline-based catalysts. When H_2 acts as the gasifying medium, coal performs hydrogasification (CHG) to generate CH_4 much more efficiently (Table 1), especially in the presence of hydrogenation catalysts. However, little review has been concentrated on this issue. (Saraceno et al. 2023) conducted a review of CHG, and the process layouts, hydrogasifiers, and catalysts were elaborated. Whereas, the catalytic mechanisms of coal hydrogasification with the addition of different catalysts (alkali-metal compounds, transition-metal compounds, and alkaline-earth-metal compounds) remain ambiguous. The profound configurations for the catalyst process (catalyst type, temperature, H_2 pressure, and coal type) and approaches for enhancing CCHG are not well understood. Moreover, it is worthwhile to analyze the industrialization prospects of CCHG further and discuss the opportunities and strategies for CCHG under the restraint of carbon neutrality.

In the present work, we systematically conducted a review dealing with CCHG for SNG production. The acting behavior of catalysts, the effect of operating conditions, and reactor configuration for CCHG are investigated. Additionally, a comprehensive outline of the process enhancement is provided based on the reaction principle of CCHG. Additionally, a brief evaluation of the CCHG process was performed, emphasizing emissions and efficiency by adopting the existing experimental results. Furthermore, novel strategies for the penetration of renewables in CCHG are proposed and preliminary validated in the context of green manufacturing. This review can help gain insights into the CCHG process and be a reliable reference for scaling up CCHG in a pressurized fluidized bed.

2 The behavior of catalysts in CCHG

2.1 Catalytic hydrogasification of model carbon

CHG integrates coal hydrolysis and coal char hydrogasification. The rate-determining step of CHG is hydrogasification of coal char, and large quantities of studies concentrated on the catalytic hydrogenation of model carbon instead of raw coal in the 1980–2010s (Hiittinger 1981; Huttinger and Krauss 1981; Holstein and Boudart 1981; Baker et al. 1982; Haga and Nishiyama 1989; González et al. 2002; Cha et al. 2007). The core of catalytic hydrogasification is to

explore the suitable catalyst with high activity, high recovery, and low cost. The catalyst commonly studied includes alkali compounds, transition compounds, and alkali-earth compounds, such as K-, Fe-, Co-, Ni-, and Ca- compounds (Qu et al. 2022). Figure 1 presents the activity of different catalysts in the hydrogasification of activated carbon (without ash, sulfur, or oxygen) at 850 °C and 1 MPa H_2 . The results show that the activity of Fe, Co, and Ni-based catalysts is much higher than that of K- and Ca-based catalysts at the loading amount of 2%. The detailed catalytic behaviors of different components are elaborated in the following sections.

2.1.1 Alkali metals

It is well known that alkali metal salts are profound catalysts for coal gasification, with water vapor as the gasifying agent (Wood and Sancier 2006). Many researchers also adopted them for hydrogasification. K- and Na-based compounds were focused because of the abundantly available source and low cost. The activity of K- compounds is in the order of $K_2CO_3 \approx KHCO_3 > K_2SO_4 > KCl$, and the activity sequence is associated with the alkalinity of potassium catalyst (Cypres et al. 1984). (Skodras et al. 2016) found that K_2PO_4 , K_2CO_3 , CH_3COOK , and KOH with higher alkalinity were more active for hydrogasification than KNO_3 , KBr , KCl , and $KHSO_4$. The added amount of alkali metals influences its activity significantly. The suitable amount of K_2CO_3 for hydrogasification is 5%–20% (as potassium metal in coal), and the catalytic reactivity generally increases with the addition of catalysts in this range (Zhan et al. 2012). When the loading amount is below 5%, the catalytic effect is not obvious because there exist few active sites, consistent with the result in Fig. 1. When the loading amount is above 20%, large quantities of catalyst would block the pore

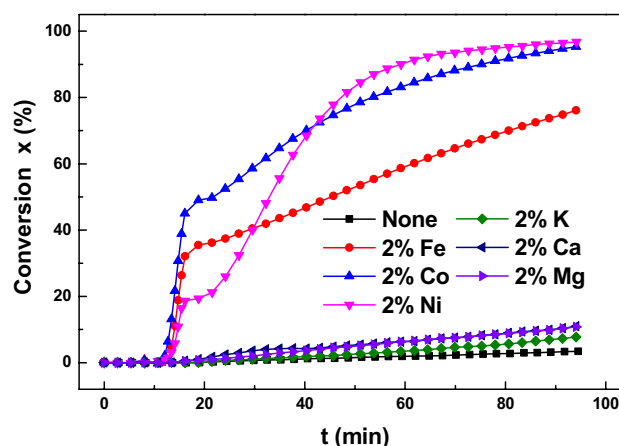
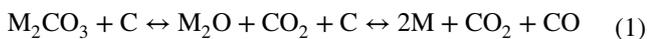


Fig. 1 Effect of different catalysts on hydrogasification of activated carbon (reaction conditions: 850 °C, 1 MPa H_2) (Qu et al. 2022)

structure and agglomerate on the surface of coal char, resulting in decreased reactivity. (Wang et al. 2019) conducted hydrogasification of coal char by blending biomass ash rich in alkali metals, and the results revealed that large quantities of K- and Na-based compounds migrated onto the coal char surface to promote hydrogasification. This research provides an economical and environment-friendly way for hydrogasification with alkali metal as the catalyst.

Different mechanisms were proposed for the alkali metal-catalyzed hydrogasification of model carbon. One mechanism involves the formation of M-(O)-C (M refers to K or Na) species during hydrogasification. (Zoheidi and Miller 1987) considered that the oxygen surface groups in coal char played an important role in determining K activity. The C=O carbonyl groups were possible candidates that would interact with K compounds to form K-(O)-C structures, which promotes CO generating and forming nascent active sites. Another mechanism is the direct reaction and interaction between model carbon and potassium compounds, as shown in Eqs. (1)–(3). (Liu et al. 2017a, b) reported that K₂CO₃ and Na₂CO₃ were reduced to K and Na metal by carbon, which then intercalated the carbon structure to restrain the graphitization process of coal char and facilitate the hydrogenation of carbon. Herein, it should be noted that the above two mechanisms might exist in hydrogasification simultaneously. (Martin and Toomajian 1992) impregnated 2%K₂CO₃ to the oxidized coal char, and a 100-fold increase in hydrogasification rate was observed. However, the same amount of K₂CO₃ results in little increase in the hydrogasification rate of activated carbon without oxygen, as shown in Fig. 1. The results hint the interaction between K and oxygen surface groups, which promotes hydrogasification significantly. When it comes to coal char with little oxygen surface groups, the catalytic hydrogasification reactivity increases with the loading amount of catalyst, suggesting that the interaction between K and carbon plays the dominant role in this circumstance.



In the CCHG process, the reaction temperature is commonly at the scope 750–900 °C, which brings about severe evaporation of the alkali compounds. (Zoheidi et al. 1987) conducted catalytic hydrogasification under 865 °C. The results showed that more than 50% of K compounds would be lost when the carbon sample gasified to 47% conversion. (Song et al. 2019) evaluated the distribution of potassium during co-pyrolysis of coal and biomass at 500 °C. They found that 65% of potassium in biomass would migrate to

the pyrolyzed coal char, 15.9% of potassium would evaporate to the gas phase, and the rest of the potassium would be retained in biomass char. Apart from evaporation, potassium tends to react with minerals in coal and form water-insoluble compounds, such as KAlSiO₄, which is catalytically inactive and causes difficulties in the recovery of potassium (Masnadi et al. 2014, 2015). Therefore, the drawbacks of alkali compounds, including the need for a large amount of catalyst additions (5 wt%–20 wt% in metal), a tendency of alkali evaporation at high temperatures, and a possibility of reacting with mineral matter, would lead to catalyst losses, high catalyst recovery costs, and the corrosion of the tubes when considering the practical application. The integration of coal and biomass hydrogasification might solve the deficiencies of alkali catalysts, as biomass is commonly rich in alkali metals, which easily migrate to coal char to promote the C–H₂ reaction. More importantly, the alkali compounds in biomass ash can be accumulated and reused cyclically without considering recovery, which might be cost-effective and fulfill the large loading amount of catalyst.

2.1.2 Transition metals

In the 1980s, (Tomita et al. 1972) first found that transition metals such as Rh, Ru, Ir, Pt, Ni, Pd, Co, and Fe possess activity towards hydrogasification of model carbon. Among them, the iron-group metals (Fe, Co, and Ni) appeal to many researchers due to their abundant resources and low price. Fe/Co/Ni supplies active hydrogen (H·), impairs the bond energy of C=C for the C–H₂ reaction and exerts profound activity with the loading of 1%–5% (Haga et al. 1987; Yan et al. 2018). As shown in Fig. 1, the activity sequence of the iron-group metals is Co ≈ Ni > Fe. However, (Ohtsuka et al. 1987; Matsumoto et al. 1991) reported that the activity order is Co >> Ni > Fe. The iron-group metals show similar capability towards supplying active hydrogen, and the key factor determining their activity is their ability to activate and fracture C=C bonds in carbon structure (Tamai et al. 1977; Yan et al. 2017). The previous results commonly found that Fe has inferior activity than Co and Ni, suggesting Fe possesses a poor endowment of breaking C=C bonds.

For Co and Ni, they exert diverse activity sequences in different studies. As each research uses the same catalyst precursor, catalyst loading amount, and reaction conditions, the discrepancy in the Co and Ni activity sequence can be correlated with using different model carbon. The carbon species were usually demineralized prior to use, and the main factor affecting the catalyst's activity might be the sulfur content. In the hydrogasification of model carbon, sulfur evolves in the form of H₂S. Plenty of research reported that a ppm grade of H₂S would suppress the activity of iron-group metals in hydrogasification because the electron

in sulfur will strongly absorb in the empty d-orbit of Co and Ni, which restrained the disassociation of H_2 and the activation of carbon structure by the catalyst (Tomita et al. 1983; Nishiyama et al. 1990). It can be seen in Fig. 2 that 50 ppm H_2S decreases the activity of Co and Ni significantly at 850 °C. With increasing the reaction temperature to a higher temperature of 950 °C, the activity of Co is recovered remarkably, while the activity of Ni remains very low. This result suggests that a higher temperature is adverse to H_2S adsorption on the catalyst surface, and the negative effect of H_2S on the Ni is more obvious than Co because H_2S is absorbed on the Ni surface more strongly.

The above discussions well explained the different activity sequences of Co and Ni in the literature. In Fig. 1, the carbonaceous material used for catalytic hydrogasification is sulfur-free, so the results present the instinct activity of Fe, Co, and Ni. (Ohtsuka et al. 1987; Matsumoto et al. 1991) use coal char as the raw material, which contains ~0.3% sulfur. A ppm grade of H_2S would inevitably be generated during hydrogasification (Matsumoto and Walker 1989), which suppressed the activity of Ni to a greater extent. Thus, Ni shows an inferior activity than Co. In terms of Fe, (Huttinger et al. 1981) found that H_2S reacted with Fe to form FeS directly instead of absorption on the Fe surface, and FeS showed no activity towards hydrogasification. For Co and Ni, no sulfide phase was formed because the Co and Ni sulfides were easily hydrogenated under a hydrogasification condition (Tomita et al. 1983; Yan et al. 2021). Instead, the generated H_2S affected their activity through strong chemical adsorption. Therefore, care should be taken when evaluating the activity of transition metals for hydrogasification of sulfur-containing materials.

Apart from H_2S , the dispersion state of iron-group metals also affects the catalytic activity, which is influenced by the

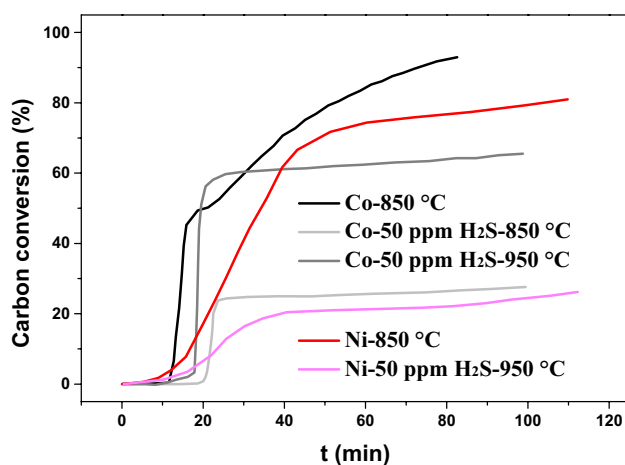


Fig. 2 Effect of 50 ppm H_2S on the activity of Co (adapted from newly experimental data) and Ni (Tomita et al. 1983) for hydrogasification

loading approach, addition amount, the catalyst precursor, et al. (Tomita et al. 1972) loaded Ni catalyst onto the activated carbon through mechanical mixing and impregnation, respectively, and the latter approach showed higher activity due to the less extent of agglomeration. The agglomeration of catalysts during hydrogasification is attributed to the following two factors: (1) The hydrogasification temperature is usually above the Tamman temperature ($T_{\text{Tamman}} = 0.5 T_{\text{melting}}$) of Fe/Co/Ni, and the bulk atoms of Fe/Co/Ni would migrate close to each other leading to agglomeration (Moulijn and Kapteijn 2001). (2) In the course of Fe/Co/Ni-catalyzed hydrogasification, the carbon gradually loses in the vicinity of catalysts, which promotes the chance of contact between the catalyst particles and results in agglomeration (Tomita et al. 1983). An increase in the loading amount of the catalyst generally contributes to the reactivity. Whereas the model carbon has a finite surface area, the agglomeration would be enhanced when the addition of catalyst exceeds the ideal amount, resulting in a decrease in reactivity. (Ohtsuka et al. 1987) investigated the effect of precursors on the dispersion of Fe catalysts. The results reveal that $FeCl_3$ and $Fe_2(SO_4)_3$ agglomerated seriously on the surface of model carbon, and the average crystallite size of Fe metals was above 100 nm. In the presence of $Fe(NO_3)_3$ and $(NH_4)_3Fe(C_2O_4)$, Fe metals were well dispersed with an average crystallite size below 29 nm. It was especially pointed out that the catalytic activity of iron-group metals decreased drastically when the average size of crystallites grew above 30 nm (Asami and Ohtsuka 1993). Therefore, the chlorides and sulfates should not act as the precursor of the catalyst. The inferior effect of chlorides and sulfates on the dispersion of catalysts was also reported in other works (Inui et al. 1979; Jiang et al. 2017).

As the iron-group metals supply active hydrogen (H) and activate $C=C$ bonds for $C-H_2$ reaction, two mechanisms exist in Fe/Co/Ni catalyzed hydrogasification of model carbon (Yan et al. 2017): (1) Active hydrogen spilling-over mechanism; (2) $C=C$ bonds breakage mechanism, as depicted in Fig. 3. It had long been vague that which mechanism plays the crucial role in catalytic hydrogasification. Matsumoto et al. (1991) found that the hydrogasification rate increased enormously upon mixing a supported Ni catalyst with the catalyst-loaded char. The result hints that the spill-over of active hydrogen promoted catalytic hydrogasification, while the role of mechanism remains unaddressed. (Tamai et al. 1977) conducted catalytic gasification in different gasifying agents (H_2O , CO_2 , or H_2), and discovered that the activity sequence of different catalysts was independent of the reactant gas. The result holds that the catalyst-carbon interaction was more important than the catalyst-gas interaction, i.e., the catalytic fracturing of $C=C$ bonds was the crucial step. As the chemisorption behavior of H_2O , CO_2 , or H_2 on different

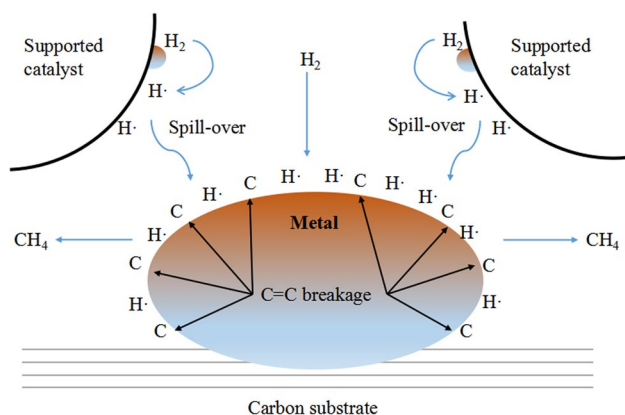
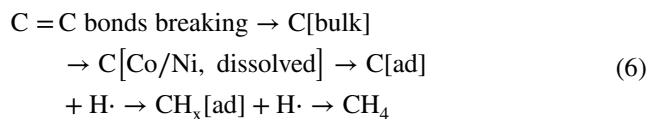
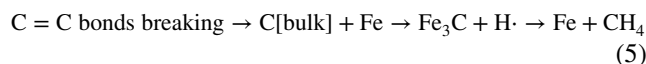
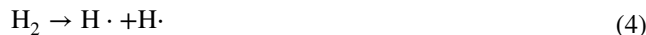


Fig. 3 The schematic diagram of Fe/Co/Ni catalyzed hydrogasification of model carbon (Matsumoto 1991; Matsumoto and Sakagami 1993)

metals is quite different, the activity sequence should have exhibited a difference if the catalyst-gas interaction was more important than the catalyst-carbon interaction. Our previous work investigated Co-catalyzed hydrogasification of coal char at different pressures, and found that the C–H₂ catalytic reaction is in zero order relative to H₂ pressure at the reaction condition of above 800 °C and 1 MPa H₂ (Yan et al. 2018). The result suggested that the supply of active hydrogen is adequate, and the catalytic fracture of C=C bonds was demonstrated to be the crucial step in the catalytic hydrogasification of model carbon. The above explorations provide meaningful theory guidance to promote catalytic hydrogasification via mediating the condensation of carbon structure instead of increasing the supply of active hydrogen under appropriate reaction conditions.

Tracing back to the instinct activity sequence of Fe, Co, and Ni, the type of interaction between the catalyst and carbon might account for their different activity, as the supply of active hydrogen is adequate at an appropriate reaction condition. Many researchers suggested that the carbide formation or carbon dissolution in Fe/Co/Ni metal might be an attractive explanation for the interaction as such carbons possessed high reactivity (Tamai et al. 1977; Holstein and Boudart 1981; Qu et al. 2019). In the catalytic hydrogasification process, Fe₃C is often found in the catalyzed coal chars, whereas no Co or Ni carbide was formed; instead, they existed in the metallic state (Yan et al. 2017; Yuan et al. 2017a, b). (Zhang et al. 2019) reported that Fe₃C is an active phase for catalytic hydrogasification, but the activity of Fe is low because the carbon atoms combined with Fe in the form of an ionic bond, which is too strong to be rapidly hydrogasified. However, in terms of Co and Ni, carbon atoms cover the catalyst surface in a dissolution state, which is readily hydrogenated by active hydrogen, and thus, Co and Ni exhibit superior activity than Fe (Haga et al. 1992;

Yan et al. 2022). Equations (4)–(6) presents the principle of Fe/Co/Ni-catalyzed hydrogasification of model carbon (Yan et al. 2017).

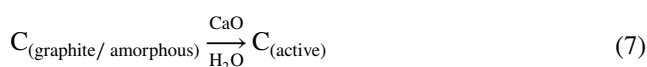


2.1.3 Alkali earth metals

Alkali earth metals such as CaO performs well in catalytic gasification with CO₂ and H₂O as the gasifying agent (Lahijani et al. 2013; Yu et al. 2020; Liu et al. 2021). In the presence of oxidizing agents, CaO was able to interact with carbon in coal and form highly reactive Ca–O–C species (González et al. 2013; Zhang et al. 2021). However, in the presence of H₂, CaO exhibited little activity toward hydrogasification of model carbon (Fig. 1). The researchers applied CaO to hydrogasification because it exerts catalytic effects on the cleavage of methyl groups in aromatic rings and accelerates the rupture of rings including BTX, PCX, indole, and benzofuran during cracking of coal tar in N₂ (Banerjee et al. 1998; Jia et al. 2004). The absence of activity for CaO-catalyzed hydrogasification might be attributed to: (1) Model carbon such as coal char and graphite has much more condensed carbon structures than the above-mentioned model chemicals. The dissociation energies of C=C bonds at the edge of condensed aromatic rings is very high because of the electron delocalization effect (Yan et al. 2022). Hence, the catalytic fracture ability of CaO may only suit the carbonaceous materials with less ordered carbon structure; (2) In the H₂ atmosphere, CaO is not able to provide active hydrogen or interact with condensed carbon, and thus it shows little activity for C–H₂ reaction (Suzuki et al. 1998).

Herein, it should be emphasized that when the model carbon is less ordered in carbon structure or contaminated by some Fe-containing minerals, the experimental result would reveal that CaO exerts profound activity toward hydrogasification. Jiang et al. (2016) conducted CaO-catalytic hydrogasification with demineralized lignite char as the raw material, and the result revealed that CaO promoted hydrogasification and restrained the graphitization process of coal char. Jiang et al. (2017) found that CaO had no activity toward hydrogasification of bituminous coal char. However, when the bituminous coal char contains a small amount of Fe, CaO would migrate adjacent to Fe, and they

cooperate to exert a catalytic effect. With the ever-ordering carbon structure to a graphite state, neither CaO nor CaO–Fe works well for hydrogasification. Casanova et al. (1983) impregnated CaO onto graphite and pretreated the specimen in an H₂O atmosphere at 600 °C prior to hydrogasification. The result revealed that CaO catalyzed the depolymerization of graphite to a more reactive form, which exhibited high hydrogasification reactivity, as shown in Eqs. (7)–(8). The above researches provide valuable strategies for enhancing CaO-catalyzed hydrogasification of model carbon, such as reducing the ordering of carbon structure, adding a definite amount of Fe, and introducing a proper content of H₂O. Anyway, it would be safe to conclude that CaO exhibits inferior activity towards hydrogasification of model carbon free of any heteroatoms.



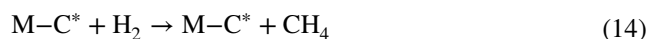
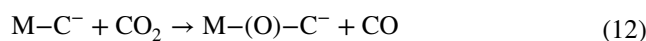
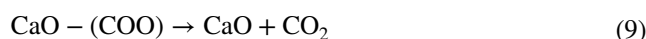
2.1.4 Transition & alkali earth bimetallic metals

The above discussions in this section indicate that the iron-group metals have advantages over the other two types of catalyst because Fe/Co/Ni possess high instinct activity for C–H₂ reaction at a low loading amount (1%–5%), and Fig. 1 shows the experimental data intuitively. However, in practical manufacturing, the carbonaceous materials (coal, coal char, pitch coke et al.) have a low surface area and a definite sulfur content. The low surface area makes iron-group metals agglomerate to form large particles, and the evolved H₂S poisons the catalyst easily, which results in the activity loss of Fe/Co/Ni towards the C–H₂ reaction.

Many efforts have been devoted to solving the sintering and poisoning problems. Among them, one efficient approach is to add alkaline-earth metals as additives (Haga and Nishiyama 1987; Dziembaj et al. 1996). Ca compound itself has little activity for hydrogasification of carbon. However, when the Ca compound acts as the additive, it not only promotes the distribution of iron-group metals on the carbon surface, but also reacts with H₂S to prevent Fe/Co/Ni from being poisoned (Yuan et al. 2015; Zhang et al. 2023). (Haga and Nishiyama 1983) investigated the effect of Ca, Mg, Al, and Ba compounds on Ni-catalyzed hydrogasification of pitch coke. The results showed that the Ca compound showed a superior promoting effect, and the ideal addition amount was 1%. Calcium nitrate and acetate have the same promoting effect, while calcium chloride shows no promoting effect.

A detailed analysis of the promoting behavior of Ca compounds revealed that the impregnated calcium nitrate/acetate reacts with carbon and forms CaO(COO) species upon heating in H₂ (Haga and Nishiyama 1983). Subsequently, CaO(COO) decomposed into CO₂ and CaO above 650 °C, which are the vital components promoting the activity of Fe/Co/Ni with Fe/Co/Ni and Ca nitrates/acetates as the precursor of the binary catalysts. (Haga et al. 1992) reported that the CO₂ liberated from the CaO(COO) would be in-situ captured by the adjacent Ni–C structure. As a result, a new Ni–(O)–C species was formed, which was responsible for the high dispersion of Ni and high reactivity of carbon. In terms of CaO, the group led by (Liu et al. 2017a, b) found that CaO not only retards Fe sintering and poisoning, more importantly, Ca also triggered Fe-catalyzing hydrogasification of low-reactive amorphous/graphite carbon. Very recently, we mechanically mixed CaO with cobalt (Co)-impregnated anthracite (Yan et al. 2021). The results showed that the CaO particles migrated to the surface of char and exhibited an enormous promoting effect on the Co-catalyzed hydrogasification of graphite carbon. When CaCO₃ was used instead of CaO, the initial reaction stage was promoted to a greater extent, attributing to the role of CO₂ evolved from CaCO₃. These experimental results validate the promoting mechanism of Ca compound proposed by (Jiang et al. 2017; Haga et al. 1992).

Therefore, the use of Ca and Fe/Co/Ni nitrates/acetates as binary catalysts solves the bottle-neck problem of iron-group metals in hydrogasification of carbonaceous resources, and the Ca compounds exhibit the following effects: (1) making Fe/Co/Ni disperse well on carbon surface; (2) retarding the poisoning of Fe/Co/Ni; (3) mediating the Fe/Co/Ni–C interactions to facilitate the catalytic hydrogenation of unreactive carbon (graphite/amorphous carbon), as shown in Eqs. (9)–(14) (Yuan et al. 2017a, b; Yan et al. 2021, 2022).



where M, C[−], and C^{*} represent Fe/Co/Ni metal, graphite/amorphous carbon, and active carbon, respectively.

Table 2 Characteristics of catalysts applied to CCHG

Catalyst type	Loading amount	Merits	Drawbacks	Catalytic mechanism
Alkali metals (K, Na et al.) (Zoheidi and Miller 1987; Liu et al. 2017a, b; Zhan et al. 2012)	5%–20%	Low price, high activity	High addition, easy to evaporate, hard to recover	Embedding into carbon structure to active carbon structure and restrain ring condensing
Alkaline earth metal (Ca) (Linares-Solano et al. 1985; Jiang et al. 2017)	2%–10%	Low price	Low activity	Activating carbon structure in the presence of H ₂ O
Iron-group metals (Fe/Co/Ni) (Matsumoto 1991; Tomita et al. 1983; Yuan et al. 2017a, b)	1%–5%	Low addition, high activity	Sintering, poisoning	Supplying active hydrogen; Impairing C=C bonds
Binary metals (Fe–Ca, Co–Ca, Ni–Ca)(Haga and Nishiyama 1987; Yan et al. 2017)	Fe/Co/Ni: 1%–5% Ca: 1%–2%	Low addition, high activity	–	Ca: promoting Fe/Co/Ni dispersion; Capturing sulfur; Mediating Fe/Co/Ni–C interaction

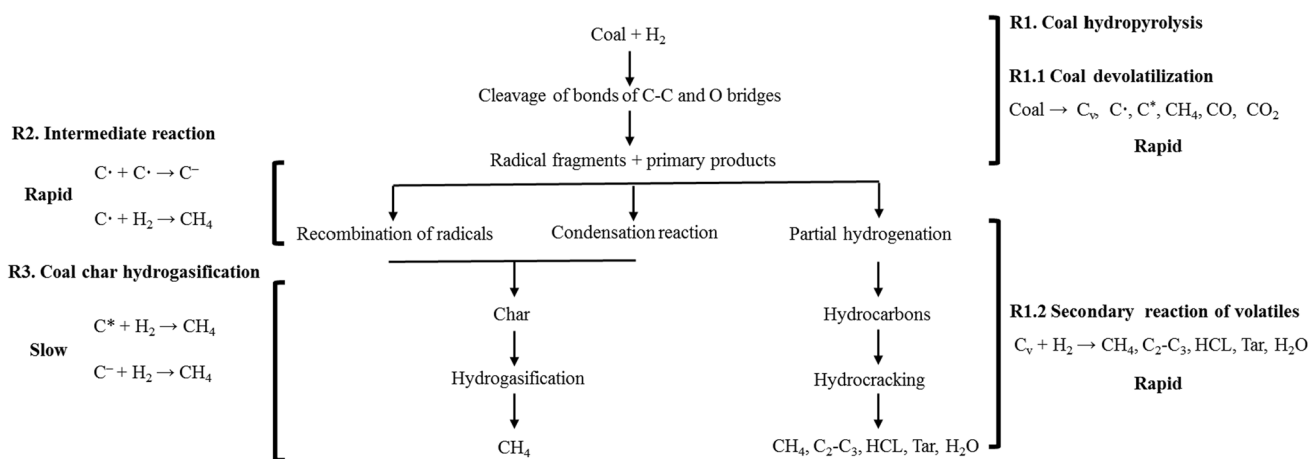
2.2 Catalytic hydrogasification of coal

Section 2.1 indicates that the rate-determining step of CHG can be well addressed by adding desirable catalysts. The behavior of different catalysts for the C–H₂ reaction is presented in Table 2. It is appreciated to observe that the binary catalyst composed of an iron-group metal and a Ca compound is superior to other catalyst types. In the course of CHG, coal particles experience devolatilization (R1.1), the secondary reaction of volatiles (R1.2), the intermediate reaction of radicals (R2), hydrogenation of active carbon, and hydrogenation of graphite/amorphous carbon (R3), as shown in Fig. 4. The previous researches on hydrogasification of model carbon primarily focused on R3. However, when it comes to CHG, the reaction process is more complicated. The catalyst not only promotes R3, but also exhibits

effects on R1 and R2, which determines the reactivity of pyrolyzed coal char and the subsequent generation of target products, including CH₄, C₂–C₃, and HCL. The researches on this issue are relatively rare because few works conducted catalytic hydrogasification with raw coal as the specimen until the past decade. In this section, the acting role of Fe/Co/Ni and Ca in the binary catalysts on CHG is elaborated with reference to the catalytic hydrogasification of model carbon and the previous works of our group on catalytic hydrogasification of coal.

2.2.1 Catalytic hydropyrolysis of coal

Plenty of works proved that Fe/Co/Ni supplied active hydrogen and impaired C=C bonds in the hydrogasification of coal char. During the hydropyrolysis of coal, the iron-group



Here C_v: carbon of volatiles, C·: carbon radicals, C⁻: graphite/amorphous carbon, C*: active carbon

Fig. 4 Reaction process of coal hydrogasification (Canel et al. 2005)

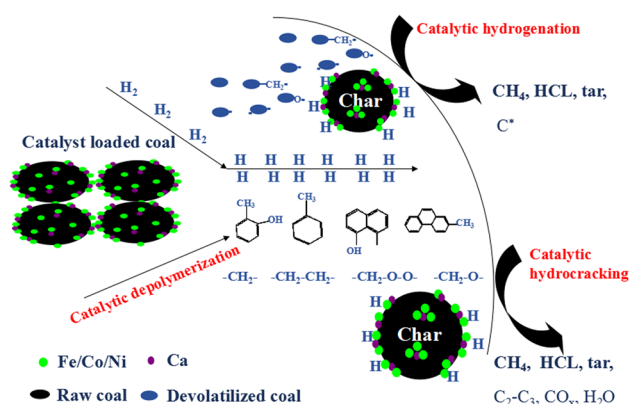


Fig. 5 Schematic diagram of the catalysis process of coal hydroxylation (Yuan et al. 2015)

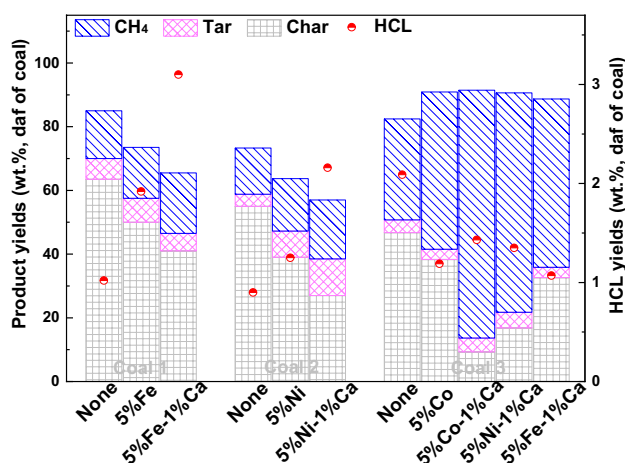


Fig. 6 Effect of catalysts on product distribution in coal catalytic hydrogasification (Coal 1 and Coal 2: subbituminous coal, conducted under 750 °C and 1 MPa H₂ by Yuan et al. (Yuan et al. 2015; Yuan et al. 2017a, b); Coal 3: subbituminous coal, conducted under 850 °C and 3 MPa H₂ by (Qu et al. 2019)

metals exerted similar effects. Two mechanisms were involved in the catalysis process, as depicted in Fig. 5. On one hand, the catalyst promoted the cleavage of chemical bonds in coal and catalyst-dissociated active hydrogen stabilized the radicals in volatiles and coal char, by which the coal devolatilization process (R1) was facilitated, and the formation of C⁻ in R2 was suppressed. This action was referred to as the catalytic depolymerization and hydrogenation mechanism (Cat-DH), which conducted to generating more volatiles and the high hydrogasification reactivity of pyrolyzed coal char (Yan et al. 2018). On the other hand, the Fe/Co/Ni-char was a strong Lewis acid structure, and it showed an enormous catalytic hydrocracking (Cat-HC) effect on the volatiles (Han et al. 2014), which decreased the tar yield and increased CH₄ yield. The combination of Cat-DH and

Cat-HC effect generally gives rise to the increase of CH₄ yield, while the tar and HCL yields depend on the behavior of catalysts, as shown in Fig. 6. In the presence of Fe or Ni, tar and HCL increased with the addition of catalyst, suggesting the Cat-DH effect plays a more important role than the Cat-HC effect. Whereas, in terms of Co, the yield of tar and HCL decreased, attributing to the extremely high acid of the Co-char structure that resulted in a severe Cat-HC effect (Yan et al. 2017; Han et al. 2014).

With the addition of 1%Ca, the tar and HCL yields for 5%Fe, 5%Ni, and 5%Co further increased. However, when 1%Ca existed alone, the tar and HCL yield decreased. This result indicates 1%Ca promoted 5% Fe/Co/Ni-catalyzed coal hydroxylation, with the promoting effect on Cat-DH being more evident than that on Cat-HC, and thus contributed to the yield of target products such as HCL and CH₄. The promoting mechanism of Ca in Fe/Co/Ni-catalyzed hydroxylation can be deduced with reference to the role of Ca in Fe/Co/Ni-catalyzed hydrogasification. It was recognized in Sect. 2.1.4 that Ca promoted the dispersion of iron-group metals, which contributed to the supply of active hydrogen and the interaction efficiency between the catalyst and coal. Additionally, Ca triggered the catalytic hydrogenation effect of Fe/Co/Ni catalyst on low-reactive amorphous/graphite carbon, suggesting the chemical bonds fracturing ability of Fe/Co/Ni catalyst was strengthened. The above roles of Ca favored the Cat-DH effect of the catalyst in hydroxylation; as a result, more volatiles were generated and hydrogenated to form CH₄, HCL, and tar (Yan et al. 2022).

2.2.2 Catalytic hydrogasification of pyrolyzed coal char

The interaction between catalyst and coal in the pyrolysis stage not only affects the formation behavior of gaseous and liquid products, but also influences the carbon structure of pyrolyzed coal char, which determines its subsequent gasification reactivity (Zhu et al. 2017; Liu et al. 2019). To facilitate coal char gasification in H₂O/CO₂, many studies impregnated catalysts onto coal surfaces and conducted catalytic pyrolysis prior to catalytic gasification. The results proved that the catalyst changed the evolution pathway of coal structure during pyrolysis. The pyrolyzed coal char was less ordering, and rich in pore structures and surface functional groups, which contributed to the high gasification reactivity (Zhang et al. 2017; Śpiwak et al. 2021). When conducting catalytic gasification in H₂, a similar role of catalyst existed. Our previous work conducted catalytic pyrolysis (in N₂) and catalytic hydroxylation (in H₂) of subbituminous coal in a pressurized fluidized bed, and the results proved that the coal char generated from catalytic hydroxylation had higher hydrogasification reactivity, as shown in Fig. 7 (Yan et al. 2018). With the coexistence of the Co-Ca catalyst and H₂ in the pyrolysis stage, the chemical bonds could be fractured

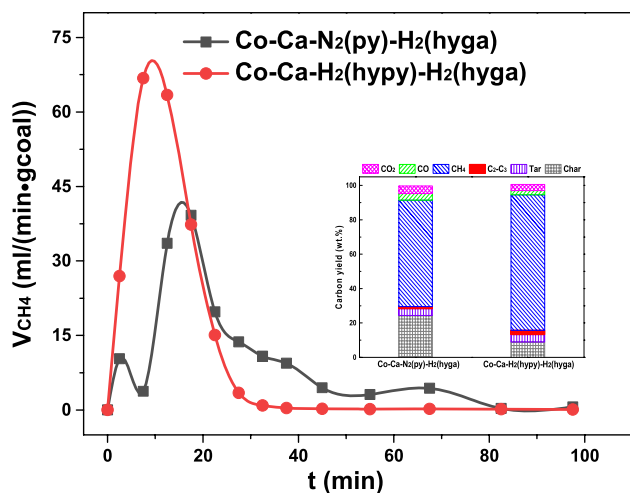


Fig. 7 Effect of coal pyrolysis on catalytic hydrogasification of pyrolyzed coal char (reaction condition: 850 °C, 3 MPa H₂; py: pyrolysis, hypy: hydroypyrolysis, hyga: hydrogasification) (Yan et al. 2018)

and hydrogenated rapidly, which had less chance to undergo ring condensation, and thus, the pyrolyzed coal char possessed more reactive sites. When H₂ was replaced by N₂ in the catalytic pyrolysis stage, the fractured chemical bonds could not be hydrogenated, which would recombine, and the condensing of coal char was inevitable; thus, the pyrolyzed coal char showed relatively low reactivity.

For the coal char generated after Co–Ca–H₂ (hypy), its subsequent catalytic hydrogasification was zero order relative to hydrogen pressure at temperatures above 800 °C

and H₂ pressure above 1.0 MPa (Yan et al. 2018; Qu et al. 2022), suggesting the supply of active hydrogen is adequate for C–H₂ reaction, and the crucial step is the catalytic cleavage of C=C bonds. The catalytic cleavage and hydrogenation process of C=C bonds has been proposed with respect to the catalysis principle of Co and the established mechanism for hydrogasification of model carbon (Calderón et al. 2016, 2017), as shown in Fig. 8. The Co catalyst embedded into the aromatic rings to facilitate the controlling step of 1,2-hydrogen migration (S2 → S3), which favored the cleavage of C1–C3 bonds and the formation rate of CH₄. In the binary catalyst system, CaO is a Lewis base, while the Co–C structure is Lewis acid. CaO appealed to migrating close to Co, making Co well dispersed and mediating the Co–C interaction, and thus, the Co-catalyzed hydrogasification of coal char was promoted. Further works are deserved to validate the stepwise catalytic cleavage and hydrogenation process of C=C bonds and reveal the interacting mechanism between CaO and Co–C structure with the aid of theory calculation.

2.3 Comparison of catalytic hydrogasification of model carbon and coal

Based on the above discussions, the characteristics of model carbon and coal catalytic hydrogasification are summarized and compared in Table 3. It can be seen that the reaction of coal catalytic hydrogasification is more complicated than that of model carbon. During this process, the superior Fe/Co/Ni–Ca bimetallic can be adopted to achieve a high CH₄ yield. According to the reaction condition, it is indicated

Fig. 8 The catalytic cleavage process of C=C bonds in aromatic rings (Yan et al. 2018)

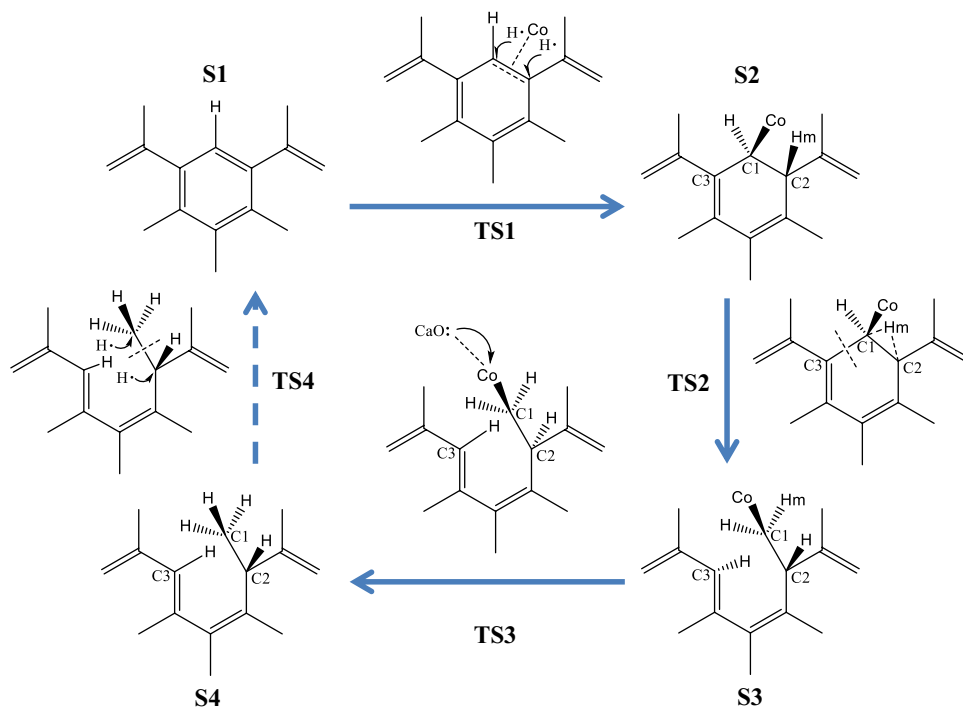


Table 3 Comparisons of catalytic hydrogasification of model carbon and coal (Haga and Nishiyama 1987; Suzuki et al. 1998; González et al. 2002; Jiang et al. 2017; Yan et al. 2017, 2022)

Comparisons	Model carbon catalytic hydrogasification	Coal catalytic hydrogasification
Reactions ^a	$C + H_2 \rightarrow CH_4$	Hydropyrolysis: $C_m H_n O_z + H_2 \rightarrow CH_4 + C_2-C_3 + CO + CO_2 + HCL + Tar + Char$ Hydrogasification: $Char + H_2 \rightarrow CH_4$
Catalysts	Fe/Co/Ni-Ca	Fe/Co/Ni-Ca
Temperature	700–1000 °C	600–850 °C
H ₂ pressure	1–7 MPa	0.1–3 MPa
Residence time	3–7 h	0.5–1 h
CH ₄ yield	50%–90%	50%–80%
HCL yield	-	1.5%–3.5%
CO ₂ emission	44.0 g/mol CH ₄	38.3 g/mol CH ₄
Energy efficiency ^b	84.5%	81.8%
Catalytic mechanism	Hydrogen spill-over C–C bonds catalytic fracturing	Catalytic depolymerization of coal Hydrogen spill-over C–C bonds catalytic fracturing

^aOnly carbon-containing products are considered in the reactions; ^bThe value of energy efficiency was calculated on the basis of 80% CH₄ yield, and the calculating method can refer to Sect. 4.3

that the hydrogasification reactivity of model carbon is much lower than that of raw coal, because higher temperature, H₂ pressure, and significantly longer particle residence time are required for model carbon to achieve a desirable CH₄ yield. Regarding CH₄ production, coal catalytic hydrogasification results in less CO₂ emission because the coal structure contains an additional amount of H; thus less ‘grey’ H₂ is required for CH₄ formation. Whereas, these additional amounts of H cause a higher heating value of coal than that of model carbon, which lowers the energy efficiency of coal catalytic hydrogasification. In terms of catalytic mechanisms, the catalysts spill over active hydrogen and impair C–C bonds for C–H₂ reaction during model carbon hydrogasification. When it comes to coal hydrogasification, the catalysts play an additional catalytic depolymerization role during the hydropyrolysis of coal. This action contributes to a higher subsequent hydrogasification reactivity of coal char and higher yields of high-value-added HCL compounds. Consequently, coal catalytic hydrogasification shows higher potential to produce CH₄ due to the relatively mild reaction conditions, higher reactivity, lower CO₂ emissions, and abundant reserves, despite the energy efficiency being somewhat lower than that of model carbon hydrogasification.

3 Effect of experimental variables on CCHG

Coal catalytic hydrogasification includes coal catalytic hydropyrolysis and coal char catalytic hydrogasification, which are greatly affected by the reaction conditions such

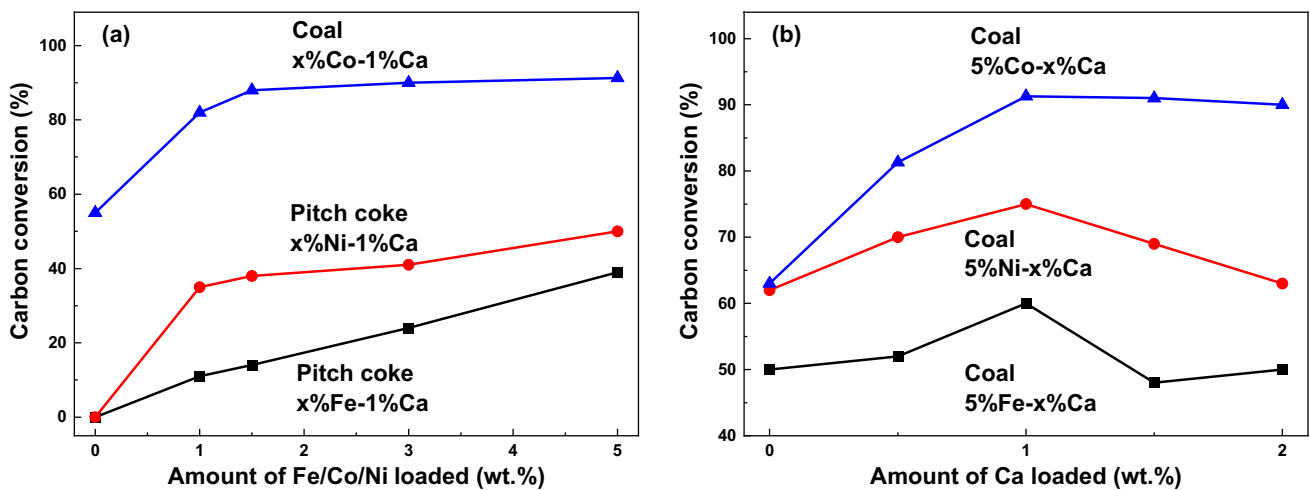
as catalyst component and amount, temperature, hydrogen pressure, coal property, et al. A clear understanding of the effect of these factors will be helpful for the design of specimen, reactor, and tailoring the generation behavior of target products (CH₄ and HCL). In the past decade, numerous researchers have concentrated on this topic, and the main results are listed in Table 4.

3.1 Catalyst type and loading

The catalyst type and loading are important parameters determining the formation efficiency of CH₄ in CCHG. The design of a catalyst should consider the activity, economy, the catalysis mechanism, et al. The selection of suitable catalyst configurations based on the above criteria and a clear understanding of the catalysis mechanisms is of significance for further researches on CCHG. It is indicated from Sect. 2.1 and Table 4 that Fe–Ca, Co–Ca, and Ni–Ca are suitable catalysts for CCHG, because they are cheaper than the noble catalysts (Pt, Ru, Rh et al.). In addition, they achieve a high yield of CH₄ in a short particle residence time (< 60 min) due to the synergy of the binary components. The role of Fe/Co/Ni is to supply active hydrogen and impaired C=C bonds in coal structure. With increasing the loading of the metals, the above behaviors will be strengthened, and the result in Fig. 9a presents that the appropriate amount might be 5%. In terms of Ca, it retards the sintering and poisoning of Fe/Co/Ni and mediates the Fe/Co/Ni–C interaction. With increasing the addition of Ca from 0% to 1%, the promoting effect increases significantly (Fig. 9b). Whereas, further increasing Ca addition from 1% to 2% decreases

Table 4 Summary of the recent research results on CCHG

Source	Specimen	Catalyst	Reactor	Conditions	Max. CH ₄ yield (%)	Max. HCL yield (%)
Hong et al. (2013)	Lignite	K ₂ CO ₃ /Na ₂ CO ₃	Fixed bed	800 °C 4 MPa	67.1 in 60 min	–
Yuan et al. (2015)	Bituminous coal	Ni/Ni–Ca	Fixed bed	750 °C 1 MPa	18.5 in 60 min	2.15
Jiang et al. (2017)	Bituminous coal char	Fe–Ca	Fixed bed	700, 750, 800 °C 3 MPa	63 in 400 min	–
Yuan et al. (2017a, b)	Subbituminous coal	Fe–Ca	Fixed bed	650, 700, 750 °C 1, 2, 3 MPa	19 in 60 min	3.38
Yan et al. (2017)	Bituminous coal	Fe–Ca/Co–Ca/Ni–Ca	Fluidized bed	850 °C, 3 MPa	77.3 in 30 min	1.32
Liu et al. (2017a, b)	Lignite char	K ₂ CO ₃ /Na ₂ CO ₃ /CaO	Fixed bed	850 °C, 5 MPa	80 in 80 min	–
Yan et al. (2018)	Bituminous coal char	Co–Ca	P-TGA	750, 800, 850 °C 1, 2, 3 MPa	88 in 60 min	–
Qu et al. (2019)	Bituminous coal	Co–Ca	Fluidized bed	850 °C 3 MPa	77.3 in 30 min	1.47
Sun et al. (2019)	Subbituminous coal char	Cu–Ni–Ca	Fixed bed	700, 750, 800 °C 2 MPa	88.3 in 450 min	–
Sun et al. (2021)	Subbituminous coal char	Cu–Ca	Fixed bed	700, 750, 800 °C 2 MPa	60.6 in 450 min	–
Yan et al. (2021)	Lignite, bituminous coal, anthracite	Co–Ca	Fluidized bed	850 °C 3 MPa	83.5 in 60 min	–
Yan et al. (2022)	Bituminous coal	Co–Ca	Fluidized bed	600, 700, 750, 800, 850 °C 0.6, 1, 2, 3 MPa	77.3 in 30 min	3.36

**Fig. 9** Effect of the loading amount of Fe/Co/Ni or Ca in the Fe/Co/Ni–Ca binary catalyst on catalytic hydrogasification (data adopted from (Haga and Nishiyama 1987; Yuan et al. 2015; Yuan et al. 2017a, b; Yan et al. 2022))

its promoting effect, attributing to the fact that the small surface area of coal particles restricts the accommodation of catalysts. Thus, a high addition of Ca gives rise to the agglomeration of Fe/Co/Ni metals (Yuan et al. 2017a, b). It is intuitively in Fig. 9 that the activity sequence of the binary catalyst is Co–Ca > Ni–Ca > Fe–Ca. The higher activity of Co–Ca might be correlated with its superior ability to

fracture C=C bonds and stronger tolerance towards H₂S during hydrogasification, as has been discussed in Sect. 2.1.2.

CH₄ is the main gaseous product in CCHG, and the increase of catalyst loading to a proper amount (Fe/Co/Ni: 5%; Ca: 1%) generally facilitates CH₄ formation rate and yield. In the binary catalyst system, the increase of Fe/Co/Ni facilitates reactions (Eqs. (4)–(6)), while the increase of Ca

promotes (Eqs. (9)–(14)), and thus they cooperate to accelerate the whole coal-H₂ reaction process. Herein, it should be noted that although adding 2%Ca has an inferior effect on the dispersion of Fe/Co/Ni than 1%Ca, the maximum CH₄ formation rate of 2%Ca was much higher than that of 1%Ca. This result is because the chemical-promoting effect of Ca on Fe/Co/Ni–C interaction was more important than the physical-promoting effect on Fe/Co/Ni dispersion (Yan et al. 2022). In the hydropyrolysis stage, Ca-promoted Fe/Co/Ni–C interaction or Fe/Co/Ni dispersion boosted the cleavage of chemical bonds in coal structure, resulting in the generation of more volatiles and the formation of pyrolyzed coal char with abundant active sites. In the hydrogasification stage, the highly dispersed Fe/Co/Ni alone was not able to catalyze hydrogenation of graphite carbon, while the Ca-promoted Fe/Co/Ni–C interaction triggered the gradual hydrogenation of graphite carbon.

In terms of liquid products such as water, tar, and HCL, their yields depend on the addition of a catalyst. The water originates from catalytic hydropyrolysis of coal and hydrogenation of nitrate/acetate catalyst, and its yield increases as the Fe/Co/Ni or Ca amount because of the hydrogenation of additional oxygen-containing catalyst precursors (Yan et al. 2018). Tar and HCL come from catalytic hydropyrolysis of coal, and the Cat-DH and Cat-HC effects dominate their yields (Yan et al. 2017). In the binary catalyst system, the two effects coexist. A high loading amount of Co (~5%) contributes to the Cat-HC effect due to the high acid of the Co–C structure, which decreases tar and HCL yield. A high loading amount of Fe/Ni (~5%) conduces to the Cat-DH effect because the acid of Fe/Ni–C structure is moderate, which increases tar and HCL yield. With increasing Ca addition to a proper amount (1%), the Fe/Co/Ni are well

dispersed, and the Cat-DH and Cat-HC effects are strengthened, with Cat-DH being enhanced to a greater extent, which favors the yield of tar and HCL.

3.2 Temperature

Reaction temperature affects the generation behavior of volatiles during the hydropyrolysis of coal, the formation rate of CH₄ during the hydrogasification of coal char, and the interaction between catalyst and coal during the reaction process. Elaborating on the effect of reaction temperature on these issues will help to tailor the CCHG process. In the

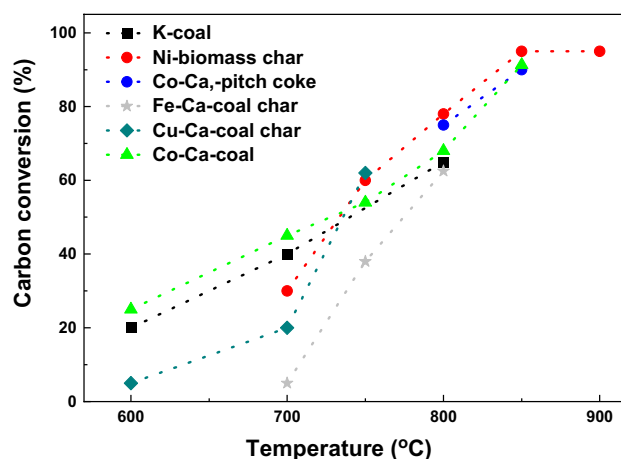


Fig. 11 Effect of reaction temperature on catalytic hydrogasification (data adopted from (Haga and Nishiyama 1987; González et al. 2002; Cha et al. 2007; Jiang et al. 2016; Sun et al. 2021; Yan et al. 2022))

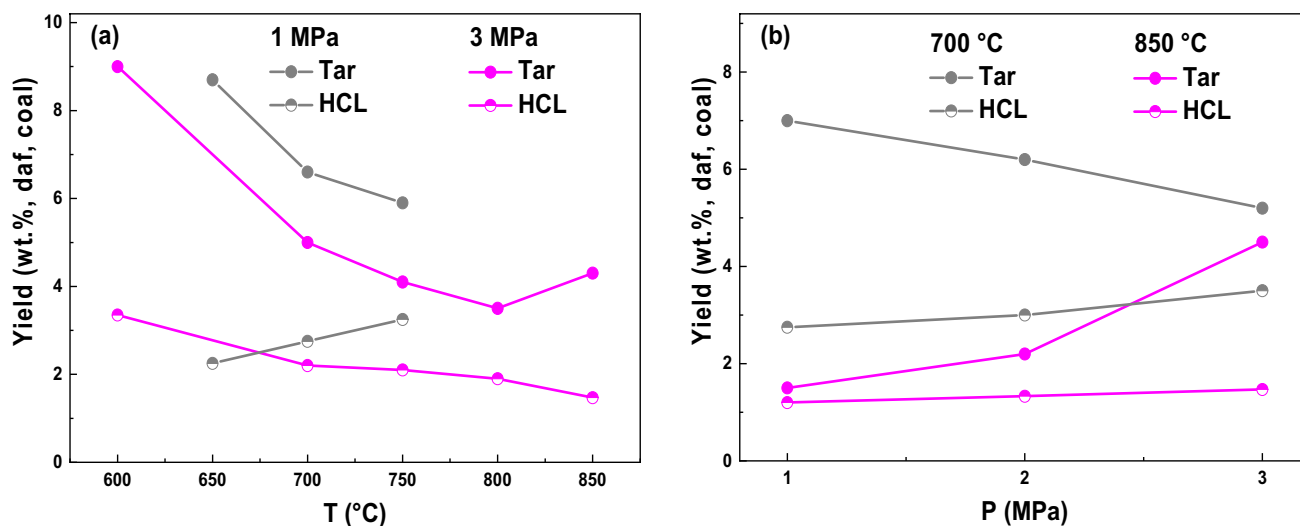


Fig. 10 **a** Effect of temperature and **b** H₂ pressure on tar and HCL yields in CCHG (data adopted from (Yuan et al. 2017a, b; Yan et al. 2022))

hydropyrolysis stage, a high temperature simultaneously promotes the Cat-DH and Cat-HC processes (Yan et al. 2022). The previous results presented that a temperature higher than 600 °C decreases the tar yield drastically because the Cat-HC effect was intensified to a greater extent, as shown in Fig. 10a. In the hydrogasification stage, the hydrogenation of carbon is the primary reaction, which is reversible and exothermic. It is consensus that a high reaction temperature is unfavorable for C–H₂ reaction due to the thermodynamic limit. However, the results in Fig. 11 show that a high temperature benefits catalytic hydrogasification, manifesting that the C–H₂ catalytic reaction locates in the kinetic-controlling region instead of the thermodynamic-controlling region at the temperature range of 600–900 °C. When the reaction temperature reaches 850 °C, more than 80% of carbon conversion (CH₄ yield) is achievable.

Reaction temperature plays two important roles in CCHG. On the one hand, a high temperature promotes the dissociation of hydrogen and the cleavage of chemical bonds. On the other hand, increasing reaction temperature facilitated the diffusion of catalyst in coal structure, which boosted the interaction frequency between catalyst and carbon; as a result, more carbon in coal was catalytically hydrogasified in much reactive form characterized by the activation energy (Yan et al. 2022). Therefore, elevating reaction temperature in the range of 600–900 °C facilitated CH₄ formation rate significantly. In general, conducting CCHG above 750 °C ensures a high coal conversion and CH₄ yield at the expense of HCL yield, as shown in Figs. 10a and 11.

3.3 Pressure

Model carbon hydrogasification belongs to a volumetric reduction reaction, and increased H₂ pressure generally

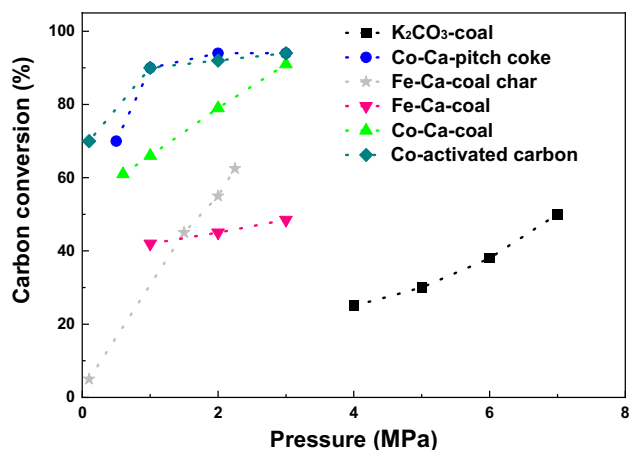


Fig. 12 Effect of H₂ pressure on catalytic hydrogasification (Haga and Nishiyama 1987; González et al. 2002; Jiang et al. 2016; Yuan et al. 2017a, b; Qu et al. 2022; Yan et al. 2022)

promotes carbon conversion and CH₄ yield. When it comes to coal catalytic hydrogasification, H₂ pressure not only affects the C–H₂ reaction, but also influences the secondary hydrogenation of volatiles during coal pyrolysis. Elaborating the effect of H₂ pressure on these issues will help to enhance CH₄ and HCL formation. As shown in Fig. 12, the increase of H₂ pressure promotes model carbon and coal catalytic hydrogasification, and most of the researchers found that a desirable CH₄ yield could be achieved by elevating H₂ pressure to 3 MPa. In the presence of a superior Co-based catalyst, a mediate pressure of 3 MPa attains a high carbon conversion of ~90%. Herein, it is worth noting that high pressure itself could not greatly facilitate coal conversion. The acting role of pressure should be accompanied by an appropriate temperature. For instance, (Yuan et al. 2017a, b) performed Fe-Ca-catalyzed coal hydrogasification at 700 °C. The results showed that carbon conversion of coal increased slightly from 42.2% to 48.0% with elevating H₂ pressure from 1 to 3 MPa. Whereas, (Jiang et al. 2016, 2017) conducted Fe–Ca-catalyzed hydrogasification of coal char at 800 °C, and carbon conversion increased significantly from 5.0% to 70.3% with H₂ pressure rising from 0.1 to 2.25 MPa. Our group also found that at a high temperature of 850 °C, the elevation of H₂ pressure from 0.6 to 3 MPa increased carbon conversion significantly from 62.1% to 91.3% for Co–Ca catalyzed hydrogasification of coal (Yan et al. 2022). The promoting effect of elevated H₂ pressure on CH₄ formation rate and yield attributes to the following facts: (i) From a kinetic point of view, large quantities of active hydrogen concentrated around the coal surface, which is appreciable for accelerating the attacking of carbon at the edge of coal; (ii) From a thermodynamic perspective, a high concentration of H₂ dilutes the CH₄ product; as a result, the reversible C–H₂ reaction proceeds to the formation of CH₄ more thoroughly.

In addition to CH₄, H₂ pressure also affects the generation of HCL, tar, CO, CO₂, et al. In the catalytic hydropyrolysis stage, high pressure, on the one hand, promoted the three-phase interaction of catalyst-coal-H₂, by which the Cat-DH effect was enhanced (Yan et al. 2022). On the other hand, rising pressure hindered the release of volatiles from the coal particle. It increased the residence time of volatiles in the high-temperature region, intensifying the Cat-HC (Zhang et al. 2014, 2016). The overall effect would give rise to the variation of HCL and tar yields in different reaction systems. When CCHG was conducted at 700 °C, the elevation of H₂ pressure promoted HCL yield while decreasing tar yield. Whereas, at a reaction temperature of 850 °C, the elevation of H₂ pressure promoted HCL yield and tar yield simultaneously (Fig. 10b), appearing that the Cat-DH was more evident than Cat-HC. This result is mainly attributed to the fact that a high temperature stimulated the diffusion of catalyst in the bulk structure of coal, and the catalytic cleavage

and hydrogenation of chemical bonds during hydrolysis were strengthened greatly, conducting to the effect of Cat-DH. In conclusion, high H_2 pressure increased the yield of HCL (Fig. 10b), while the yield of tar depends on the reaction temperature. In terms of CO and CO_2 , a high H_2 pressure promoted the methanation and reversal water–gas shift reactions, and thus, the CO and CO_2 as byproducts decreased at the elevated pressure.

3.4 Coal property

The above reviews mainly concentrated on catalytic hydrogasification characteristics of model carbon or idealized coal with low ash, low caking index, low sulfur content, and medium–low rank. However, in the practical production process, the exploited coal usually has one or more of the abovementioned properties, which might influence the instinctive activity of catalysts. For instance, Ni-catalyzed hydrogasification of biomass char achieved a high carbon conversion of 95% at a moderate reaction condition of

850 °C and 0.1 MPa H_2 (González et al. 2002). Whereas, for Ni-catalyzed hydrogasification of pitch coke at 850 °C and 1 MPa H_2 , only ~10% carbon conversion was achievable (Haga and Nishiyama 1987). The discrepancy in Ni activity mainly arose from the carbonaceous specimen's different carbon structures or sulfur content. (Jiang et al. 2017) performed Fe-catalyzed hydrogasification of coal char prepared from the same bituminous coal. The results revealed that the un-thoroughly demineralized char showed higher reactivity as the retained CaO-containing ash promoted Fe activity greatly. Therefore, elaborating the effect of coal properties on CCHG and exploring the process mediating approaches are important for the further application process.

To address this issue, a comprehensive investigation of catalytic hydrogasification of coals with high ash, caking propensity, high rank, or sulfur content was conducted in a pressurized fluidized bed very recently (Yan et al. 2021). The results in Fig. 13 show that CCHG can adapt well to medium–low rank coals with low caking index and low sulfur content directly, and the high ash content has limited

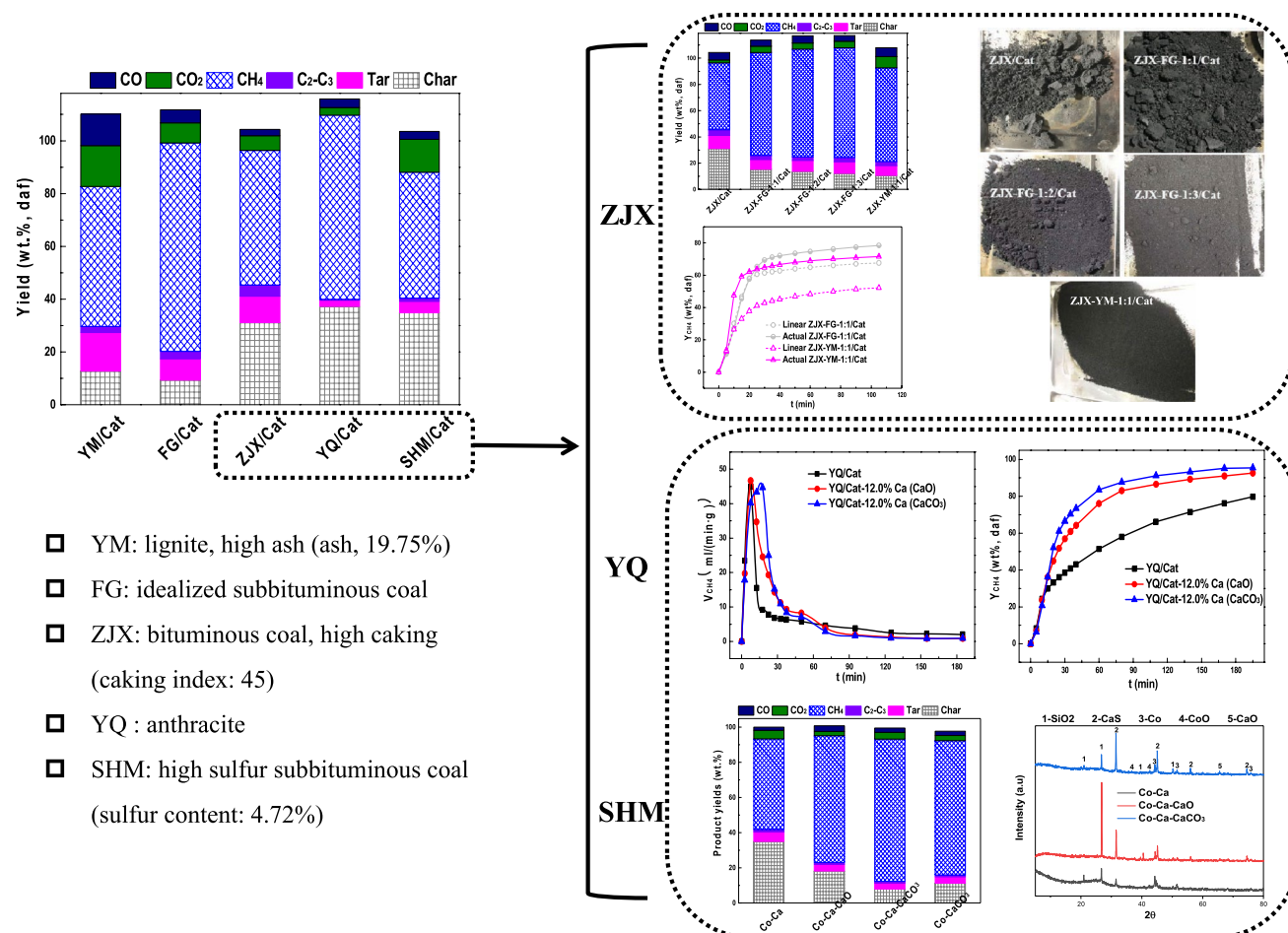


Fig. 13 Catalytic hydrogasification characteristics of coals with diverse properties in a pressurized fluidized bed (reaction condition: 850 °C, 3 MPa H_2) (Yan et al. 2021)

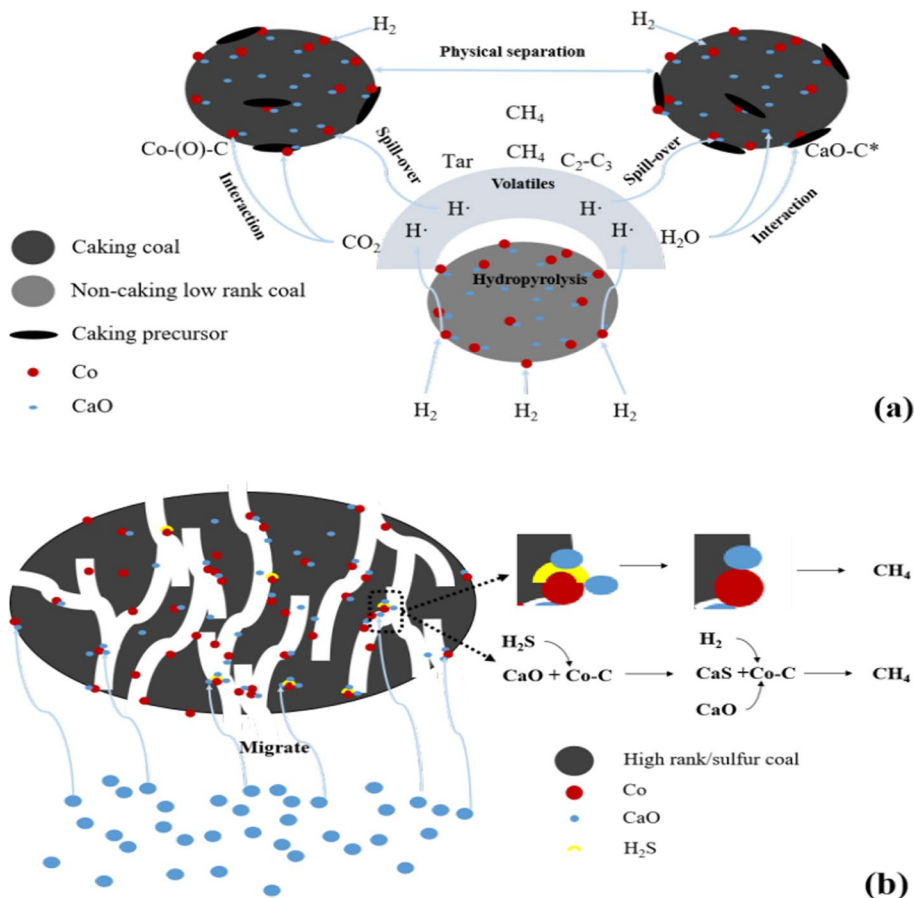
residence to the activity of the catalyst. However, a suitable mediation approach should be adopted to realize a high reactivity in terms of high caking, high rank, or high sulfur-containing coal.

For CCHG of high caking ZJX coal, the blending of a definite amount of medium–low rank FG coal or YM coal not only well addressed its caking propensity due to the physical separation effect, but also greatly promoted the overall CCHG reactivity because of the volatile-catalyst-coal interactions as shown in Fig. 14a, correspondingly, Eqs. (7), (8), (12)–(14) in Sect. 2.1 depicted the interaction process. When it comes to CCHG of high-rank YQ anthracite and high sulfur-containing SHM subbituminous coal, the mechanical blending of a suitable amount of CaO/CaCO₃ promotes the reactivity enormously. On the one hand, CaO/CaCO₃ migrated into the pore structures of coal to trigger the activity of iron-group metals towards hydrogenation of inert carbon in coal; on the other hand, CaO/CaCO₃ captured H₂S during CCHG to retard the poisoning of iron-group metals, as depicted in Fig. 14b. The promoting role of CaO/CaCO₃ can also be interpreted by the proposed mechanism in Eqs. (9)–(14).

3.5 Impurities in gasifying agent

It is noteworthy that in a practical production process, CCHG in a continuous gasifier might not implemented in pure H₂, but in the mixture of H₂, H₂O, CO₂, CO, H₂S, et al., because coal-generated H₂O, CO₂, CO, and H₂S affects CCHG. (Feng et al. 2023a) investigated the effect of steam on Co–Ca-catalyzed coal hydrogasification, and the results demonstrated that the presence of 5% steam in the gasifying agent significantly inhibited Co–Ca activity toward hydrogasification. The negative effect of steam could be relieved by elevating the reaction temperature to 900 °C and total pressure. However, other researchers evidence the promoting effect of steam on CCHG. For instance, (Casanova et al. 1983) found that water vapor initiated the CaO-catalyzed depolymerization of graphite/amorphous carbon; thus, carbon in coal existed in a more reactive form and was easily hydrogenated. (McKEE 1974) demonstrated that water vapor in H₂ significantly promoted Fe-catalyzed hydrogasification of graphite. The discrepancy in the effect of H₂O on CCHG might attributed to the type of catalyst and reaction

Fig. 14 Schematic diagram of probable mechanisms for catalytic hydrogasification of **a** Caking coal and **b** High rank/sulfur coal (Yan et al. 2021)



conditions, and further researches should be conducted to clarify the effect of H₂O comprehensively. In terms of CO and CO₂, (Gil and Smoliński 2015) proved that adding 10% CO₂ to H₂ considerably enhanced char hydrogasification. Our previous work (Feng et al. 2022) conducted CCHG in H₂+CO₂, and the results demonstrated that Co–Ca containing char improved the CH₄ selectivity of CO/CO₂ methanation, thus significantly increasing coal-based CH₄ production. When it comes to H₂S, it is consensus that the ppm grade of H₂S poisons Fe/Co/Ni catalysts during CCHG (Matsumoto and Walker 1989; Yan et al. 2021). The negative effect of H₂S can be mitigated by elevating the reaction temperature to above 900 °C or adding AAEMs additives (Huttinger and Krauss 1981; Tomita et al. 1983; Yan et al. 2021). A high temperature restrains the strong absorption of H₂S on the catalyst surface, and the AAEMs are conducive to react with H₂S to form sulfates, by which the poisoning effect of H₂S could be eliminated. The above experimental results provide theory guidance to modulate hydrogasification reactivity when conducting CCHG in complicated gasifying conditions.

3.6 Methods for promoting CH₄ and HCL in CCHG

In the context of CCHG, it has been noted that the generation of target products (CH₄ and HCL) closely correlates with the reaction conditions, including the catalyst type, catalyst loading, reaction temperature, H₂ pressure, coal property, etc. In terms of catalyst, 5%Co–1%Ca showed higher activity than that of 5%Ni–1%Ca and 5%Fe–1%Ca as cobalt had a superior performance for activating C=C bonds in coal structure, which facilitated coal depolymerization to boost HCL formation and enhanced coal char hydrogasification

to accelerated CH₄ formation. For reaction conditions, it is consensus that a high temperature is not beneficial for CH₄ yields because a positive standard Gibbs free energy change (ΔG^\ominus) will emerge. However, plenty of research conducted CCHG at a high temperature of around 800–1000 °C, and high CH₄ yields could be obtained (Mısırlıoğlu et al. 2007; Yan et al. 2002; Fan et al. 2023). Herein, it is of interest to ascertain how reaction conditions affect C–H₂ reaction. Figure 15 shows the thermodynamic results for the effect of temperature and pressure on the C–H₂ methanation reaction. It can be seen that a high temperature decreases CH₄ yield in all cases. Nevertheless, when a high temperature is coupled with high pressure, CH₄ yield can be boosted to a great extent. Especially at a high C:H₂ ratio of 1:4 under 5 MPa, achieving a 100% CH₄ yield at 900 °C is possible. This result can be interpreted by Eqs. (15)–(16). At a high reaction temperature, ΔG^\ominus is a positive value. When a high hydrogen pressure or C:H₂ molar ratio is accompanied, the term $RT \ln J$ would be negative because the value of J will be much less than 1. As a result, a negative value of ΔG can be obtained under a high temperature. The thermodynamic results explain well why CCHG experiments are usually implemented under high temperatures and H₂ pressure. A high temperature is beneficial to accelerate the methanation reactions, while a high H₂ pressure or high C:H₂ feeding ratio is conducted to achieve a desired equilibrium state for CH₄ yield.

$$\Delta G = \Delta G^\ominus + RT \ln J \quad (15)$$

$$J = \frac{P_{\text{CH}_4}/P^\ominus}{(P_{\text{H}_2}/P^\ominus)^2} \quad (16)$$

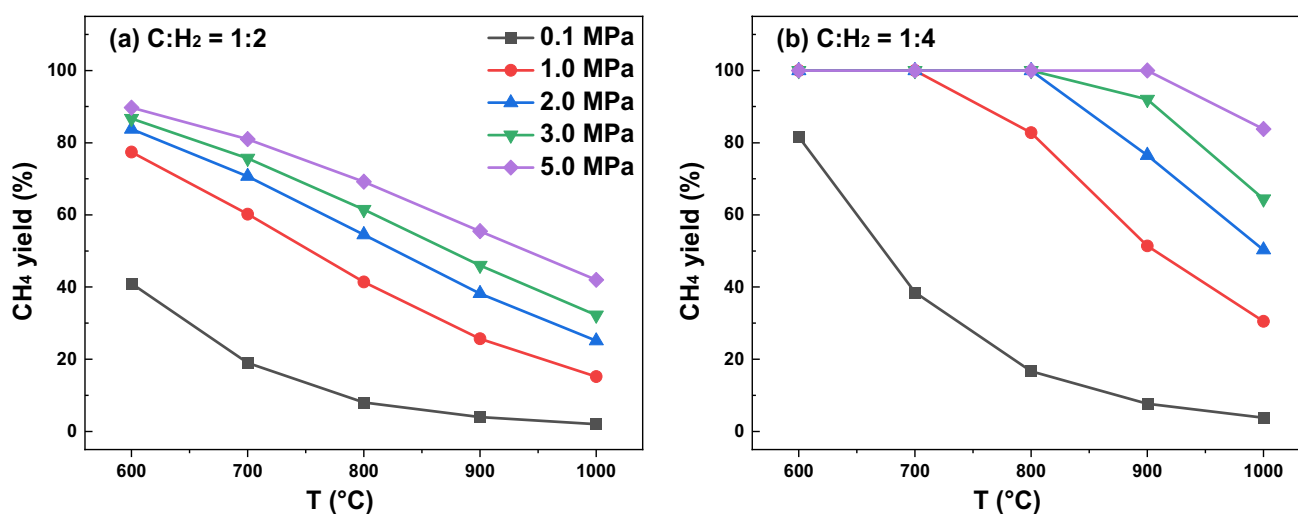
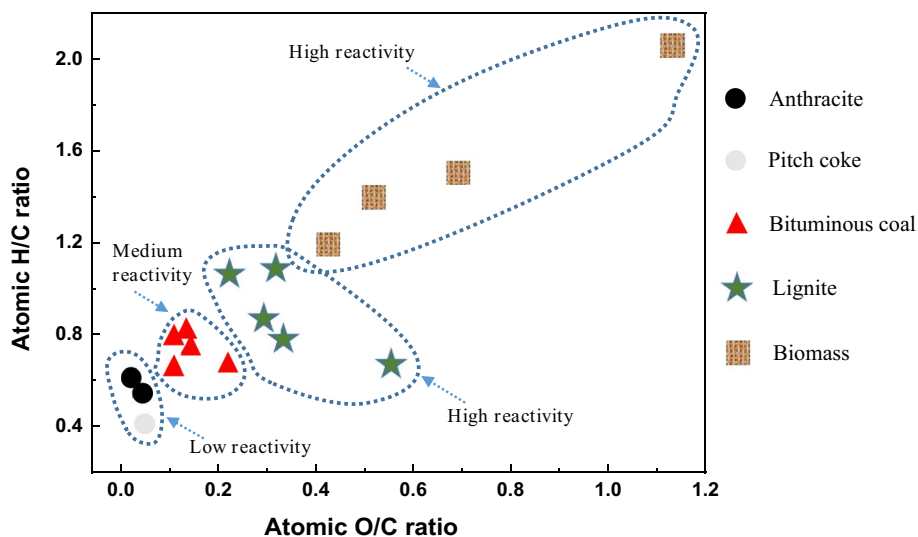


Fig. 15 Thermodynamic results of CH₄ yield from C–H₂ reaction with varying reaction conditions a C:H₂ molar ratio of 1:2 b C:H₂ molar ratio of 1:4

Fig. 16 Ther Van Krevelen diagram of various hydrogasification feedstocks (data adopted from (Haga and Nishiyama 1987; Ohtsuka et al. 1987; Zhan et al. 2012; Hong et al. 2013; Zhang et al. 2016; Tian et al. 2021; Yan et al. 2021))



wherein, ΔG is Gibbs free energy change at certain reaction conditions, J/mol; R is the universal gas constant, J/(mol K); T is the reaction temperature, K; J is the reaction quotient; P_{CH_4} is CH₄ partial pressure, Pa; P_{H_2} is H₂ partial pressure, Pa; P^θ is standard pressure, Pa.

Figure 16 depicts the Van Krevelen diagram of various hydrogasification feedstocks. The results show that the feedstocks with higher atomic O/C and H/C ratios perform superior reactivity. The higher atomic O/C ratio is suggestive of abundant oxygen-containing species in carbon structure (Zoheidi and Miller 1987; Zhao et al. 2020), and a higher atomic H/C ratio represents that more edge carbon persists (Tomeczek and Gil 2010), and they are commonly recognized as active sites for hydrogasification or catalytic hydrogasification (Zoheidi and Miller 1987; Yan et al. 2018). Therefore, when considering CCHG feedstocks,

medium–low rank coals (lignite and subbituminous coal) and biomass with high atomic O/C and H/C ratios are preferred. Apart from these feedstocks, recent works also demonstrated that CCHG could be applied to coals with high ash/caking/rank/sulfur properties. Through the modulating approach of blending low-rank coal or CaO/CaCO₃, high carbon conversion (~90%) and CH₄ yield (~80%) were achievable in a short particle residence time of 1.0 h (Yan et al. 2021). These results manifested that the technology of CCHG has the potential to act as a universal method for carbonaceous resources (coal, pitch coke, biomass, solid wastes, et al.)-to-SNG. The effects of experimental variables on CCHG are summarized in Table 5, and the results might provide valuable proposals for regulating target products and dealing with different kinds of carbonaceous feedstocks.

Table 5 Effect of experimental variables on CCHG

Item	Range	Acting behavior	Promoting strategy
Catalyst type (Haga and Nishiyama 1987; Yan et al. 2017)	Fe–Ca, Co–Ca, Ni–Ca	Ideal loading: 5%Fe/Co/Ni–1%Ca Activity sequence: Co–Ca > Ni–Ca > Fe–Ca	–
Temperature (Yan et al. 2022)	600–850 °C	A high temperature promotes CH ₄ yield, but decreases HCL yield	Two stage bed under high pressure: Stage 1, low temperature, boost HCL; Stage 2, high temperature, boost CH ₄
H ₂ pressure (Yuan et al. 2017a, b)	0.1–3 MPa	A high H ₂ pressure promotes CH ₄ and HCL yields	
Coal property (Yan et al. 2021)	High ash/caking/rank/sulfur	Medium–low rank coals show high CCHG reactivity Coal ash does not retard catalyst activity; Caking propensity arises agglomeration; High rank coal has low CCHG reactivity; Sulfur poisons Fe/Co/Ni catalyst, and 1%Ca is insufficient to capture high content of H ₂ S	Blending low rank coal or biomass: retard agglomeration, promote reactivity; Blending CaO/CaCO ₃ : promote Fe/Co/Ni activity, retard poisoning

4 Preliminary evaluation of CCHG process

In the CCHG process, the recovery of the catalyst, the emission of the pollutants, the thermal efficiency of the reaction, and the scaling-up perspective are important issues to be concerned. To date, the abovementioned subjects have yet to be addressed comprehensively. This section discussed the Co–Ca-catalyzed coal hydrogasification, focusing on the recycling of Co, the generation behavior of nitrogen/sulfur-containing species, the thermal analysis, and the scaling-up calculation of the whole reaction process preliminarily.

4.1 Recycling of catalyst

In the Co–Ca-catalyzed coal hydrogasification process, Co catalyst existed in metallic form without reacting with the inherent minerals (Qu et al. 2019). Hence, the expensive Co can be recovered by a simple acid leaching method. The result in Fig. 17 shows that a high recovery of 99.9% can be realized for Co, and the recycled catalyst obtained comparable activity with the fresh catalyst. For the laboratory scale of CCHG, the nitrates commonly act as the precursor of catalysts. However, when it comes to the commercial scale of CCHG, large quantities of HNO_3 and nitrates would be used. In China, the commercial scale of utilizing nitrates may be prohibited in policy due to the susceptible of

preparing explosives; thus, another alternative catalyst for nitrate should be explored.

Tracing back to the catalyst loading process, the Co salts should be impregnated onto the coal to attain a good dispersion, while the Ca compound could be loaded by wet-impregnation or mechanically mixing (Yan et al. 2021). Therefore, it requires that the Co salts are water-soluble. In addition to nitrates, relatively cost-effective salts such as cobalt acetate, halides, and sulfates are optional. However, (Inui et al. 1979; Feng et al. 2023b) reported that the halides and sulfates easily agglomerated and showed low activity during hydrogasification; thus, only cobalt acetate is available. Figure 18 shows the characteristics of CCHG with acetates with the catalyst. Compared to 5%Co–1%Ca-nitrate, 3%Co–1%Ca-acetate has a comparable carbon conversion, CH_4 formation rate, and yield. In terms of tar and HCL, their yields are 7.8% and 2.2%, respectively, much higher than that of 4.04% and 1.5% for 5%Co–1%Ca-nitrate. Therefore, using acetates as a catalyst precursor in CCHG has an advantage over the nitrates as a lower loading amount of Co achieves a higher yield of target products.

The Co catalyst in the char residue can be recovered through acid leaching-precipitation-acid dissolving, as shown in Fig. 18c. The recovery of Co in this procedure also reaches 99.9%, and the recovered $\text{Co}(\text{Ac})_2$ and $\text{Ca}(\text{Ac})_2$ can be re-impregnated onto the coal to conduct CCHG. The

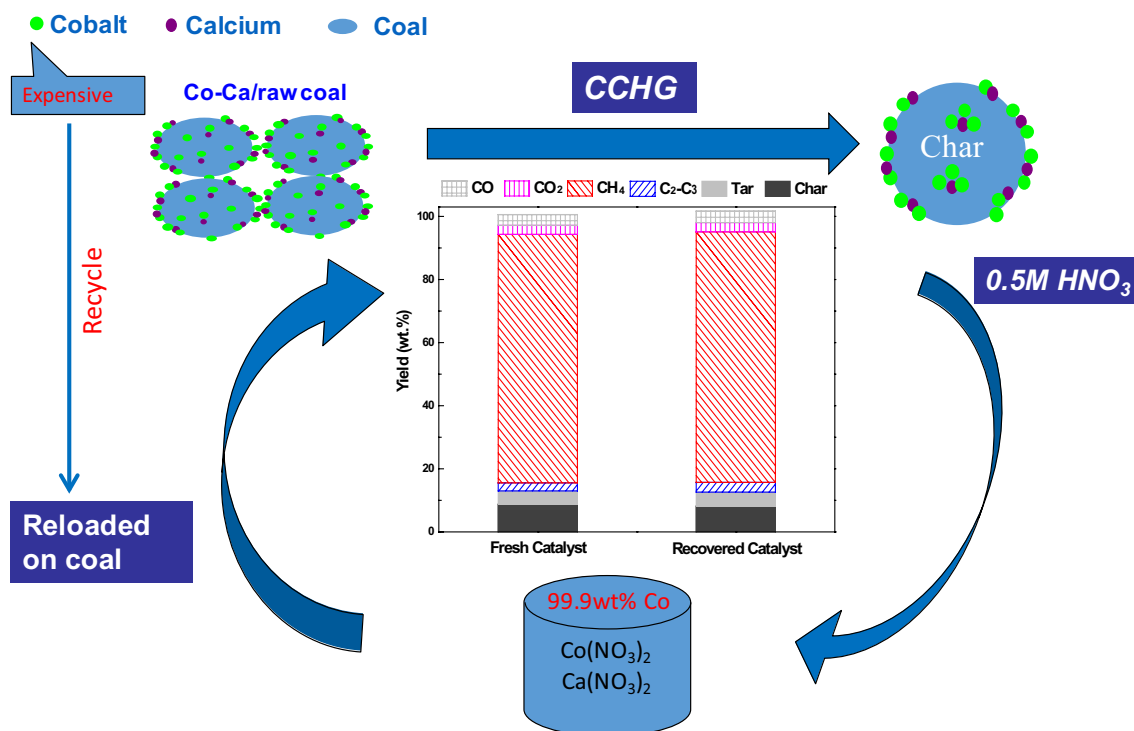


Fig. 17 The schematic diagram of recycling Co catalyst for CCHG (Yan et al. 2017)

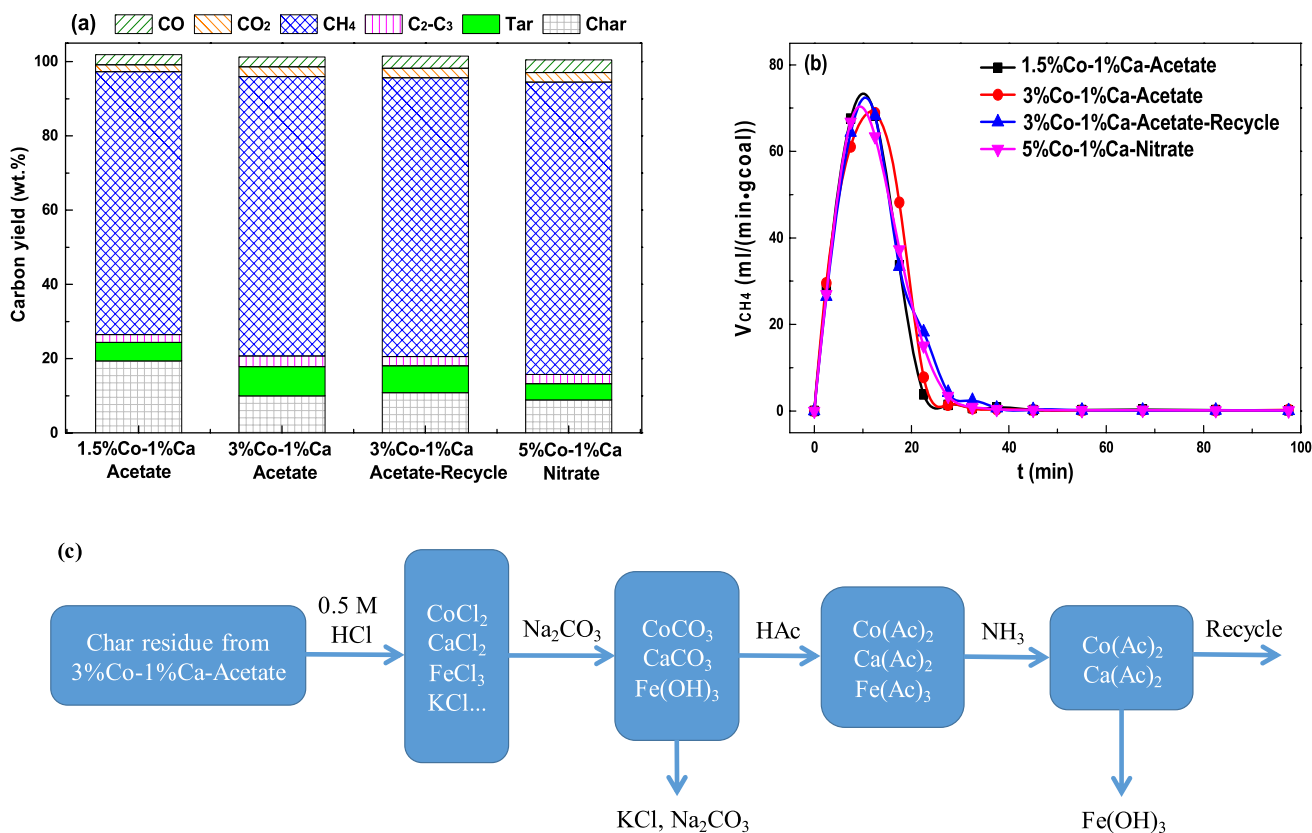


Fig. 18 Catalytic hydrogasification of coal with acetates as the precursor of catalyst **a** Products distribution **b** CH₄ formation rate **c** Recovering process of Co and Ca acetates (reaction condition: reaction condition: 850 °C, 3 MPa H₂, recovery condition: 25 °C)

results in Fig. 18a and b show that the activity of the recovered catalyst changes insignificantly. Herein, it is worth noting that the recycling of the catalyst was conducted only once, far less than the required cycles for the practical production process. In the long run, some inherent coal minerals will inevitably be dissolved into the catalyst precursors and then influence Co–Ca activity. To address this issue, our recent work investigated the effect of seventeen mineral impurity elements on Co–Ca-catalyzed coal hydrogasification (Feng et al. 2023b). The results demonstrated that a high Co recovery of 99.7% could be obtained after six cycles, while the activity of Co–Ca catalyst was not able to be maintained because Al and S-containing compounds performed a negative effect on Co–Ca activity. Relevant results will guide the optimization of catalyst recycling and the reusing process by removing the impurities.

For instance, the negative effect of Al can be eliminated by modulating the catalyst recovery process. (Feng et al. 2023b) penetrated the sodium jarosite precipitation technology into the Co recovery process, as shown in Fig. S1. The results prove that more than 95% of Al will be removed into jarosite at a pH of 4.0. As a result, the activity of the

recovered catalyst nearly rebounded to the level of the fresh catalyst, which showed great potential for application. In terms of S-containing compounds, they mainly reacted with Ca salts and thus lowered the synergy catalytic effect between Co and Ca. This effect could be mitigated by adding extra CaO/CaCO₃ into the CCHG system, as it had been demonstrated that the physically mixed CaO/CaCO₃ could migrate into the cobalt-loaded char and promote the activity of Co enormously (Yan et al. 2021).

4.2 The emission of sulfur/nitrogen-containing species

SO_x, H₂S, NO_x, HCN, et al. are the commonly reported pollutants in coal gasification, with steam, CO₂, or O₂ as the gasifying agent (Yuan et al. 2012; Duan et al. 2017). However, under a catalytic hydrogasification condition, the formation behavior of sulfur and nitrate species is not well documented, especially in the presence of a catalyst. For sulfur-containing species, (Tomita et al. 1983; Liang et al. 2016) reported that sulfur in coal was mainly generated in the form of H₂S during CCHG, which poisoned

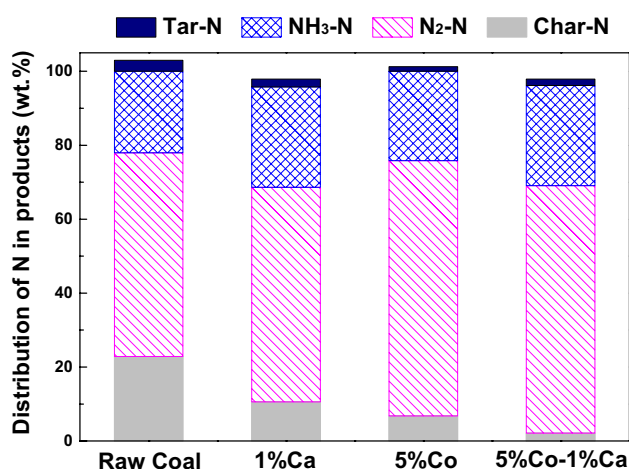


Fig. 19 The mass balance of nitrogen in CCHG (reaction condition: 850 °C, 3.0 MPa H₂; Total nitrogen = nitrogen in coal + nitrogen in nitrate catalyst; ‘Tar-N’, ‘NH₃-N’, ‘N₂-N’, and ‘Char-N’ refer to the distribution of nitrogen in Tar, NH₃, N₂, and coal char, respectively) (Yan et al. 2022)

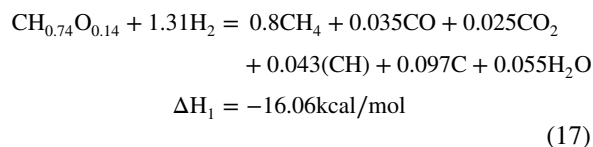
the iron-group metals. Very recently, our group conducted Co–Ca-catalyzed hydrogasification of high-sulfur coal (Yan et al. 2021). The results revealed that the mechanically mixed CaO in a fluidized bed could capture the evolved H₂S, and the gaseous products contained no sulfur-containing species detected by the mass spectrometry, suggesting that the CCHG process possesses an important characteristic of generating no sulfur-containing pollutants in the gaseous products.

In terms of nitrogen-containing species, it can be seen in Fig. 19 that nitrogen in coal and nitrate catalysts mainly evolved in the form of N₂ and NH₃, tar-N and char-N during CCHG, while no NO_x was detected by using the equipment of NO_x analyzer (NO_x5210). In the presence of a Co–Ca catalyst, more than 95% of N was converted into N₂ and NH₃ with an NH₃ selectivity of 28.8%, and the detailed analysis of products found that nearly all NH₃ dissolved in the condensed water. Preliminary experimental results revealed that the CCHG-to-SNG process is an environmentally friendly process without generating nitrogen or sulfur-containing pollutants in gaseous products. Moreover, the nitrogen in coal and catalyst precursors can be resourced into a valuable product of ammonia, which can potentially complement the ammonia synthesis process.

4.3 Thermal efficiency

Based on the available experimental data for CCHG, the thermal efficiency can be preliminarily evaluated. The basic data is presented in Table 6, and the following calculation procedure is adopted with reference from (Steinberg 2005):

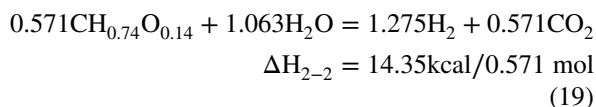
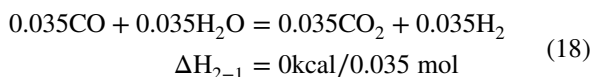
- (1) Catalytic hydrogasification of FG bituminous coal



wherein, the automatic ratio of C, H, and O is calculated based on the ultimate analysis; the CH₄ is assumed to be the sum products of CH₄ and C2–C3 in Table 6; (CH) is assumed to be the tar; C is referred to as char.

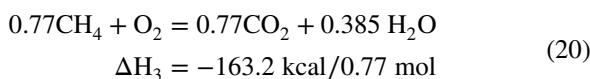
In terms of reaction heats, the coal pyrolysis stage is assumed to be 1.14 kcal/mol, while the heat released for generating CH₄ in the hydrogasification stage is –17.2 kcal/0.8 mol CH₄, calculated based on the stoichiometric reaction of C + H₂ = CH₄ (ΔH = –21.5 kcal/mol). Therefore, the overall reaction heat for CCHG is –16.06 kcal/mol (ΔH₁).

- (2) Hydrogen production



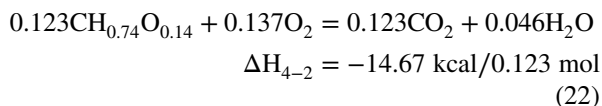
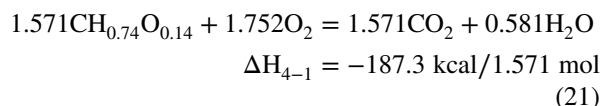
wherein, 1.31 mol H₂ for CCHG comes from the water–gas shift reaction and coal gasification; The raw material is 0.035 mol CO generated from CCHG and 0.571 mol FG bituminous coal, respectively. The overall reaction heat for H₂ production is 14.35 kcal/mol (ΔH₂).

- (3) Lower heating value (LHV) of CH₄ product



wherein, it is assumed that 0.03 mol CH₄ of equivalent energy is used for catalyst recovery; thus the net CH₄ production is 0.77 mol.

- (4) LHV of raw coal



wherein, the 1.571 mol CH_{0.74}O_{0.14} is supplied for hydrogasification and hydrogen production, while the combustion of 0.123 mol CH_{0.74}O_{0.14} is used for

Table 6 Primary experimental data for calculating the thermal efficiency of CCHG (Yan et al. 2022)

Sample	Ultimate analysis (wt%, dry-ash free basis)					Product yields (wt%, carbon basis)						
	C	H	N	S	O	CH ₄	C2–C3	CO	CO ₂	Tar	Char	
FG bituminous coal	78.7	4.9	1.2	0.4	14.8	77.3	2.5	3.5	2.6	4.4	8.7	

compensating the endothermic gasification reaction in procedure 2).

(5) Overall thermal efficiency

The ratio of output energy to input energy is the overall thermal efficiency, which can be calculated as follows:

$$\text{Thermal efficiency} = (\Delta H_1 + \Delta H_2 + \Delta H_3) / (\Delta H_{4-1} + \Delta H_{4-2}) = 81.8\%$$

Preliminary results reveal that compared to other coal-to-SNG technologies in Table 1, CCHG not only harvests a higher yield of CH₄, but also has higher thermal efficiency that in turn mitigates CO₂ emission. Therefore, scaling up CCHG is feasible to reduce the emissions (SO_x, NO_x, and CO₂) for SNG production, which fulfills the context of green manufacturing.

4.4 Suitable gasifier for CCHG

Table 7 presents the characteristics of different reactors commonly applied to coal gasification, including fixed bed gasifier, fluidized bed gasifier, entrained bed gasifier, and plasma gasifier (Chanthakett et al. 2021; Midilli et al. 2021). A fixed bed reactor is usually adopted for the fundamental

research of CCHG, because it is capable of dealing with a small dose of coal sample to ensure the reproducibility of the results, collecting the gas–liquid–solid three-phase products, and attaining the instinct reaction kinetics. Whereas, the fixed bed reactor might not be the suitable gasifier, as CCHG treats pulverized coal (< 6 mm) instead of lump coal (6–50 mm) for impregnating catalyst. In addition, CCHG is a strongly exothermic reaction, and the large quantities of reaction heat might be hard to remove in situ, resulting in the flying of temperature and the sintering of the catalyst.

When it comes to the fluidized bed reactor, pulverized coal can be used, and the reaction temperature of 800–1000 °C, pressure of 10–30 bar, and minute-level particle residence time can all be suited to CCHG. The pulverized coal particles used for impregnation of catalysts, an appropriate reaction temperature and H₂ partial pressure (850 °C, 3 MPa) favor the activity of catalysts, and the minutes of reaction time is necessary for achieving a high carbon conversion and CH₄ yield. It is consensus that the fluidized bed has a profound transferring endowment, which promises good temperature-controlling ability and makes CCHG proceed fluently (Xia et al. 2021). Moreover, as indicated in Sects. 3 and 4, CCHG in a pressurized fluidized bed can be well adapted to coals with diverse properties, and it produces SNG with little toxic emissions. Therefore, CCHG in a fluidized bed gasifier overcomes the drawback of a fixed bed

Table 7 Characteristics of different gasifiers (Chanthakett et al. 2021; Midilli et al. 2021)

Reactor type	RZT (°C)	Pressure (bar)	PS (mm)	PRT	Characteristics
Fixed bed gasifier	500–1000	1–100	6–50	Hour level	Stepwise hydrogenation of coal Long residence time Hard to remove reaction heat
Fluidized bed gasifier	800–1000	1–50	0.15–6	Minute level	Use pulverized coal Easily scaling up Good temperature control
Entrained bed gasifier	900–1600	20–80	<0.15	Second level	Short residence time Flexibility on coal types Hard to impregnate catalyst
Plasma gasifier	Up to 10,000	20–80	No requirement	Second level	Needless of catalyst Short particle residence time Low emissions of carbon and toxics Requirement of high cost and frequent maintenance

RZT Reaction zone temperature, PS Particle size, PRT Particle residence time

gasifier; simultaneously, the advantages of the entrained bed gasifier (flexibility on coal types) and plasma gasifier (low emission of carbon and toxins) are also taken.

4.5 Coupling of reaction and fluidization process underlying scaling-up of CCHG

When conducting CCHG in a fluidized bed gasifier, H_2 acts as not only the gasifying agent, but also the fluidization medium, which leaves open questions about the integration of reaction and fluidization. That is, in the context of a scaling-up process, the feeding H_2 should make the coal particles well fluidized and thoroughly converted by obeying the following criteria: (1) the fluidizing number (N) locates in 2–5; (2) the ratio of dense-phase bed height (H) to the inner diameter of fluidized bed (D) is 2–5; (3) the mass of H_2 to the mass of coal is 0.25–0.67 to ensure a sufficient supply of H_2 and high utilization of hydrogen atom. Wherein, H_2 /Coal (mass ratio, referred to as ‘ r ’) of 0.25 is the stoichiometric hydrogen for the C– H_2 methanation reaction, while r of 0.67 is the value used for generating the products in Table 6, and it is considered as the upper-limit for supplying H_2 . Thus, N and H/D are associated with fluidization, while the value of r correlates with the reaction, and these values should be well coupled.

In the context of scaling-up of CCHG in a fluidized bed, there are many independent variables to be ascertained to fulfill the above-mentioned requirement, consisting of coal particle diameter (d_p), reactor diameter (D), fluidizing number (N), and mass feeding rate of coal (W). By taking the results in Table 6 as the basis for scaling up CCHG, the known experimental variables and the restrictions for designing the fluidized bed are listed in Table 8. In the commercial scale of CCHG, the value of d_p is estimated to be 2 mm for pulverized coal, while the value of D is determined as 3.6, 3.0, and 2.5 m in the calculation process. The calculating procedure is shown as follows:

1. Minimum fluidization velocity (u_{mf})

The Ergun equation is used for calculating the minimum fluidization velocity of coal particles (Chitester et al. 1984):

$$Re_{mf} = \frac{\rho_g d_p u_{mf}}{\mu_g} = -\frac{k_2}{2k_1} + \sqrt{\left(\frac{k_2}{2k_1}\right)^2 + \frac{1}{k_1} Ar} \quad (23)$$

wherein, ρ_g is H_2 density, kg/m^3 ; μ_g is H_2 viscosity, $Pa\cdot s$; $k_2/2k_1 = 28.7$, $1/k_1 = 0.0494$, and Ar is the Archimedes constant.

2. Fluidization velocity (u) and mass feeding rate of coal (W)

$$u = N \cdot u_{mf} \quad (24)$$

Table 8 The CCHG conditions and restrictions for scaling-up of CCHG in a fluidized bed

<i>Conditions</i>	
Gasifying agent	H_2
Reaction temperature T	850 °C
System pressure P	3.0 MPa
H_2 viscosity μ_g	0.0000212 Pa·s
H_2 density ρ_g	0.64 kg/m^3
Coal particle size d_p	2 mm
Coal particle density ρ_s	1400 kg/m^3
Particle residence time T	30 min
Bed inner diameter D	2.5, 3.0, 3.6 m
<i>Restrictions</i>	
Fluidization number N	2–5
H_2 /coal mass ratio r	0.25–0.67
Dense-phase bed height H	2–5 D

$$W = \frac{2u\pi D^2}{4 \times 22.4r} \quad (25)$$

Generally, W can be determined to produce a definite amount of SNG per year from CCHG. For instance, Table 6 indicates that 1.2 $Nm^3 CH_4$ can be generated from 1 kg coal in CCHG. Accordingly, to produce 2 billion cubic CH_4 from CCHG per year, 5400 t/d coal should be handled. Based on the determined W , the u and r can be determined with varying N (2–5). Meanwhile, the value of H can also be ascertained according to Eqs. (26)–(28).

3. Bed expanding height

(Babu et al. 1978) proposed an equation taking into account high-pressure expansion data shown as follows:

$$\frac{H}{H_{mf}} = 1 + \frac{1.957(u - u_{mf})^{0.738} d_p^{1.006} \rho_p^{0.376}}{u_{mf}^{0.937} \rho_g^{0.126}} \quad (26)$$

$$H_{mf} = \frac{4W \times t}{3.14 \times 1000D^2 \rho_s (1 - \epsilon_{mf})} \quad (27)$$

$$\epsilon_{mf} = Ar^{-0.21} (18Re_{mf} + 0.36Re_{mf}^2)^{0.21} \quad (28)$$

wherein, H_{mf} is the bed expanding height at the minimum fluidization velocity, m ; ρ_p is the coal particle density, kg/m^3 ; t is the residence time of coal particle, h ; ϵ_{mf} is the bed voidage at the minimum fluidization velocity; Re_{mf} is the Reynolds number at the minimum fluidization velocity.

Figure 20 presents the calculating results for scaling-up of CCHG in a fluidized bed using Eqs. (23)–(28). It can be seen that with the increase of D , the capacity of the fluidized bed increases at the precondition that the values of

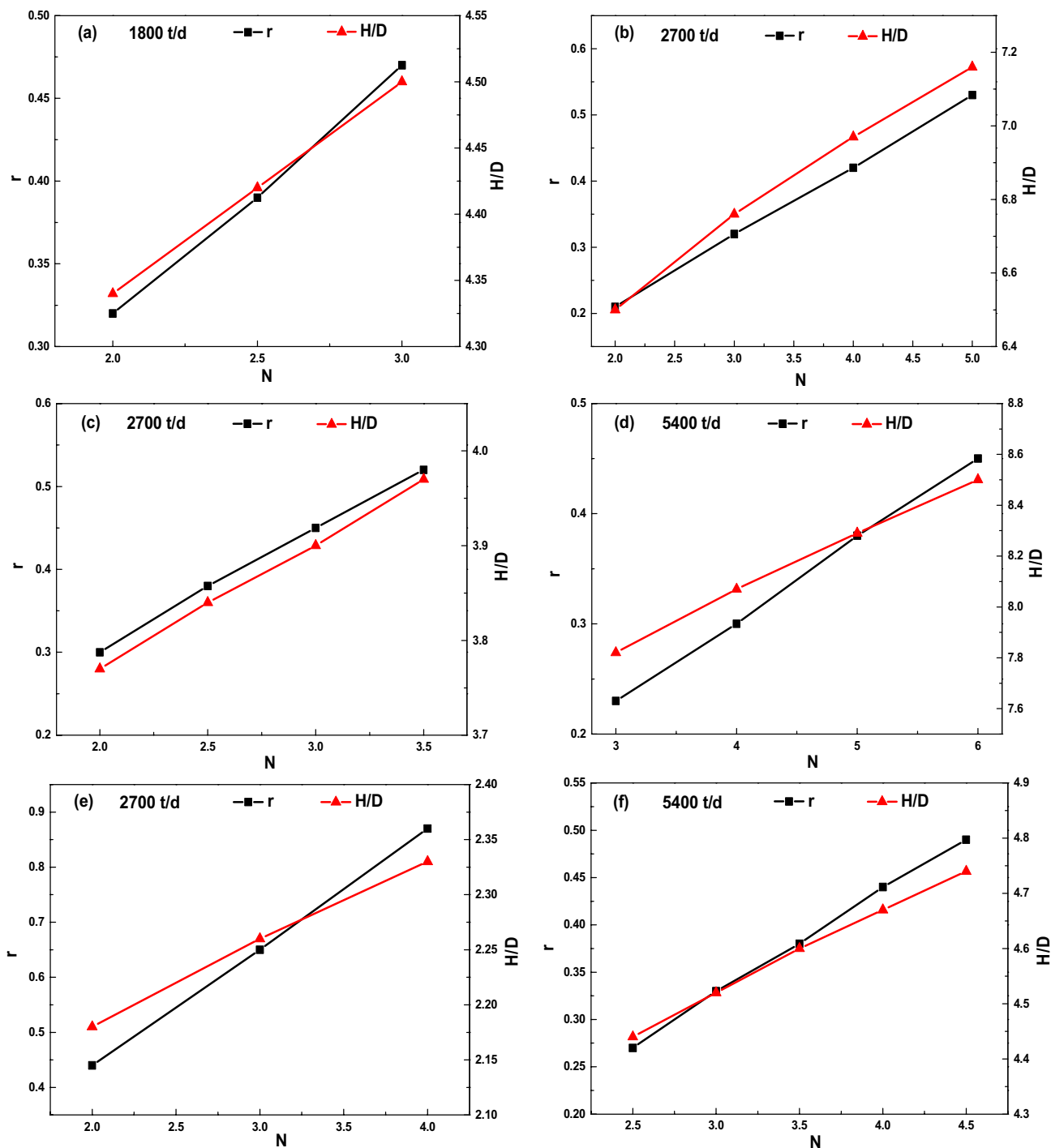


Fig. 20 The calculation results for scaling-up of CCHG in a pressurized fluidized bed **a**, **b** $D=2.5$ m **c**, **d** $D=3.0$ m **e**, **f** $D=3.6$ m

N , r , and H/D are located in the appropriate range of 2–5, 0.25–0.67, and 2–5, respectively. For the diameter of 2.5 m, the handling of 1800 t/d coal is capable as N , r , and H/D are well coupled (Fig. 20a). With increasing the capacity to 2700 t/d, the value of H/D exceeds the range of 2–5 (Fig. 20b), which might be inappropriate. Figure 20c and

d show that the reactor diameter of 3.0 m can deal with 2700 t/d coal, while unable to handle 5400 t/d coal due to the high H/D ratio. 3.6 m is the upper limit for designing the diameter of a fluidized bed reactor in practical application, and this value makes the reactor capable of handling 2700–5400 t/d coal, as shown in Fig. 20e and f. This result

might be striking because it means that 2 billion cubic SNG can be produced in one gasifier dealing with 5400 t/d coal.

Tracing back to the coal-to-SNG technologies in Table 1, CCG and CCHG have attracted wide attention in recent years because of their high thermal efficiency, high CH_4 yield, and short process. In the commercial coal-to-SNG process, the production of 2 billion cubic SNG/year is the minimum limit, which requires 12 fluidized bed gasifiers (2 gasifiers for standby) for CCG, and 5 fluidized bed gasifiers for CCHG with 2 gasifiers for generating SNG (1 gasifier for standby) and 3 gasifiers for supplying H_2 (1 gasifier for standby). The much fewer gasifiers needed for CCHG attributes to the fact that much more CH_4 is produced from an equal amount of coal as compared to CHG, which exhibits a great perspective for the investment of facilities. If demonstrated, CCHG in a pressurized fluidized bed with pulverized coal as the raw material has the potential to act as a complement for the mature two-stage gasification (Lurgi technology) with lump coal as the raw material.

5 Opportunities and strategic approaches for CCHG

5.1 Opportunities

While there are numerous pressures with the utilization of fossil fuels in the context of carbon neutralizing, there exist many opportunities for innovative gasification technologies that are clean, thermally efficient, and able to reduce the environmental impact. Of the existing coal-to-SNG technologies, the release of CO_2 in the CCHG process is estimated to be $1.71 \text{ kg/Nm}^3 \text{ CH}_4$, much lower than that of commercialized Lurgi technology ($4.03 \text{ kg/Nm}^3 \text{ CH}_4$) and demonstrated CCG technology ($3.22 \text{ kg/Nm}^3 \text{ CH}_4$) from a reaction point of view (Chen et al. 2017). Moreover, CCHG, with a higher efficiency of up to 81.8%, may have an additional contribution to reducing greenhouse gas emissions. From an environmental perspective, CCHG generates little nitrogen/sulfur-containing pollutants in gaseous products, and thus, applying CCHG for SNG production might minimize the damage to nature.

The conventional Lurgi process generates large amounts of ash and waste exposed in products other than gases, needing further disposal (Yang et al. 2017). When the SNG production process is done with CCHG, the solid and liquid products can be used as resources. For instance, there remains 8.7 wt% carbon unable to be converted in the CCHG process (Table 6), and detailed analysis of the remaining carbon reveals that it is characterized by large

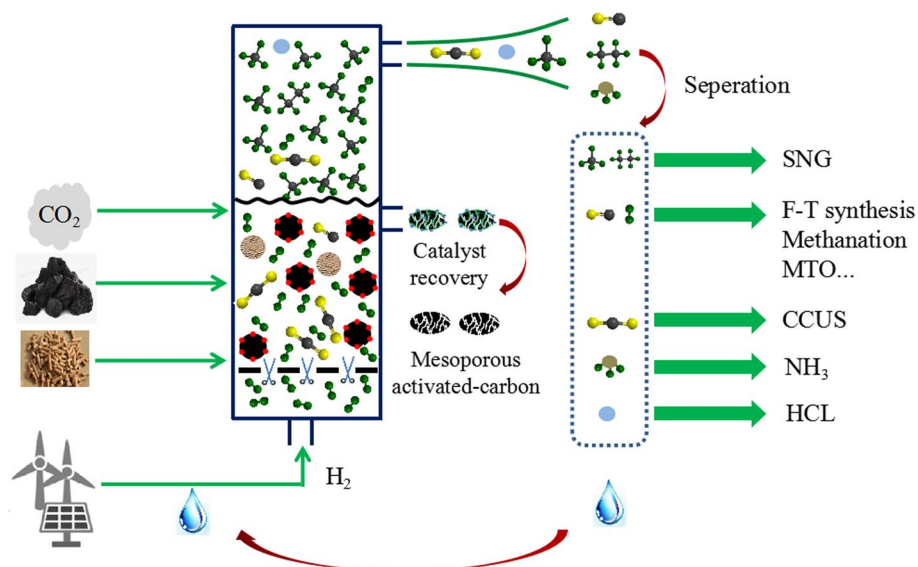
amounts of reactive sites and dominated mesoporous structure with a high surface area of $409 \text{ m}^2/\text{g}$ after recovering of the catalyst (Qu et al. 2019). These properties make it possible to be used as a profound raw material, catalyst, or carrier in the field of tar upgrading (Chen et al. 2020), flue gas desulfurization (Song et al. 2017), catalytic graphitization (Liu et al. 2013), CO/CO_2 methanation (Ipsakis et al. 2021), microwave absorbents (Liang et al. 2022), et al. In terms of liquid products, CCHG is able to produce 3.36 wt% HCL as a byproduct (Table 6), and it can be used as valuable chemicals. In addition, the dissolved NH_3 in the water product (Sect. 4.2) can also be resourced. It can be estimated that CCHG generates $\sim 66,000$ tons of HCL and $\sim 16,478$ tons of NH_3 along with 2 billion cubic SNG per year in one fluidized bed gasifier, which may be an important aspect making the economy of the process favorable.

5.2 Strategic approaches

The investment of CCHG strongly depends on the availability of low-cost hydrogen. Coal gasification is the mature H_2 production process in China and other countries mainly relying on imported natural gas, which generates a large amount of CO_2 ($\sim 1 \text{ kg CO}_2/\text{Nm}^3 \text{ H}_2$) (Jin et al. 2022). It is noteworthy that today, partly H_2 can be obtained from renewable sources, including biomass, wind, and solar (Bargiacchi et al. 2021; Valizadeh et al. 2022; Lu et al. 2023; Ghodke et al. 2023). Renewable energy-initiated electrolysis has a modest effect on the environment, and the CO_2 emission is below $0.18 \text{ kg CO}_2/\text{Nm}^3 \text{ H}_2$ (Tosti et al. 2016), much lower than that of the coal gasification-to- H_2 process. (Glenk and Reichelstein 2019) established a model and predicted that in the next ten years, the power to gas technologies would produce renewable H_2 with costs competitive to the gasification process. The model also predicted that the policy incentives could make renewable H_2 more economical in places like Texas and Germany. In this regard, the renewable H_2 acts as an intermediate “energy vector” for CH_4 , and CCHG produces SNG with an extremely low CO_2 emission of $\sim 0.4 \text{ kg CO}_2/\text{Nm}^3 \text{ CH}_4$. As a result, CCHG-based SNG is not only an attractive, versatile energy carrier for coal, but also stores surplus power from renewables in off-peak hours, which promotes the penetration of renewables and fossils in future energy systems.

Figure 21 presents a schematic description of the future possibilities of CCHG technology. The “green” H_2 generated through renewable energies is an important medium for hydrogenating carbonaceous resources, including coal, biomass, CO_2 , etc. By the approach of CCHG, the carbonaceous resources can be converted into useful chemicals and materials such as SNG, synthesis gas, NH_3 , HCL, and activated carbon with mesoporous structure. The recovered catalyst and

Fig. 21 Technology routes for future perspectives of CCHG



condensed water can be recycled for impregnation and electrolysis. Herein, it is noteworthy that anticipated by the global urgent for reducing CO₂ emissions and the market need for SNG in Asian and EU countries, the CCHG technology is not only a service for merely one carbonaceous resource, but may be able to deal with multi-carbonaceous resources, such as co-CCHG of coal and biomass, co-CCHG of coal and CO₂, et al. To date, the catalytic hydrogenation of individual coal, biomass, or CO₂ has already been studied (Zhou et al. 2020; Wang et al. 2022). Whereas, few researches, to the best of our knowledge, have provided an analysis on the coupled CCHG of coal and biomass, or coal and CO₂, with H₂ as the gasifying agent. It may be meaningful to gain some insights into this issue because implementing renewables and the penetration of CO₂ utilization in coal catalytic hydrogasification helps mitigate carbon emissions in the context of SNG production. To this end, our group investigated co-catalytic hydrogenation of coal and biomass/CO₂ in a pressurized fluidized bed very recently (Yan et al. 2021; Feng et al. 2022), and preliminary results are shown in Figs. 22 and 23.

5.2.1 Co-CCHG of coal and biomass

Biomass is a carbon-neutral feedstock with high reactivity, and it can be hydrogasified without adding a catalyst (Tian et al. 2021). We preliminarily conducted biomass hydrogasification and co-CCHG of biomass and coal in a fluidized bed, and the experimental details are presented in Methodology S2. As shown in Fig. 22, biomass hydrogasification achieves a high conversion of 90.1% and generates a considerable amount of CO (27.5%), SNG (30.6%), and tar (3.88%). Despite the profound results, the large-scale hydrogasification of biomass is impractical due to the low energy density and the restricted seasonal availability. In this regard,

co-CCHG of coal and biomass provides a strategy for clean and efficient utilization of fossil fuel and renewable energy.

As shown in Fig. 22a, the penetration of 20 wt%–30 wt% biomass into CCHG yields comparable results with coal catalytic hydrogasification. The results in Fig. 22b show that adding 20 wt%–30 wt% biomass into CCHG greatly decreases the generation of byproducts, including CO and CO₂, reaffirming co-CCHG is a low-carbon-emission process. Detailed analysis of CH₄ formation behavior in Fig. 22c and d reveals that biomass promotes coal catalytic hydrogasification remarkably. Especially at the addition of 30%, the maximum CH₄ formation rate for the experimental result is 1.94 times that of the linear result, indicating an intensive interaction between biomass and catalyst-containing coal during co-CCHG. The promoting effect might be attributed to the role of alkali & alkaline earth metals in biomass or the transferring of large quantities of radicals with low molecules from biomass to coal (Ellis et al. 2015; He et al. 2021; Wang et al. 2021; Wu et al. 2021). Further researches are needed to elaborate the interaction mechanism clearly, which will help provide theory guidance for the design of specimens and enhance the CCHG process by adopting a cheap and disposable Fe-Ca catalyst.

5.2.2 Co-catalytic hydrogenation of coal and CO₂

The transformation of CO₂ to valuable chemicals such as CO and CH₄ using renewable H₂ has proven to be an emerging solution to mitigate climate change and global warming (Saeidi et al. 2021). The in-depth research on this process is consistent with the European policy with the target of reducing 80% of greenhouse gas emissions compared to 1990 levels by 2050 (Ipsakis et al. 2021), Chinese policy to peak greenhouse gas emissions by 2030 and reach carbon-neutral

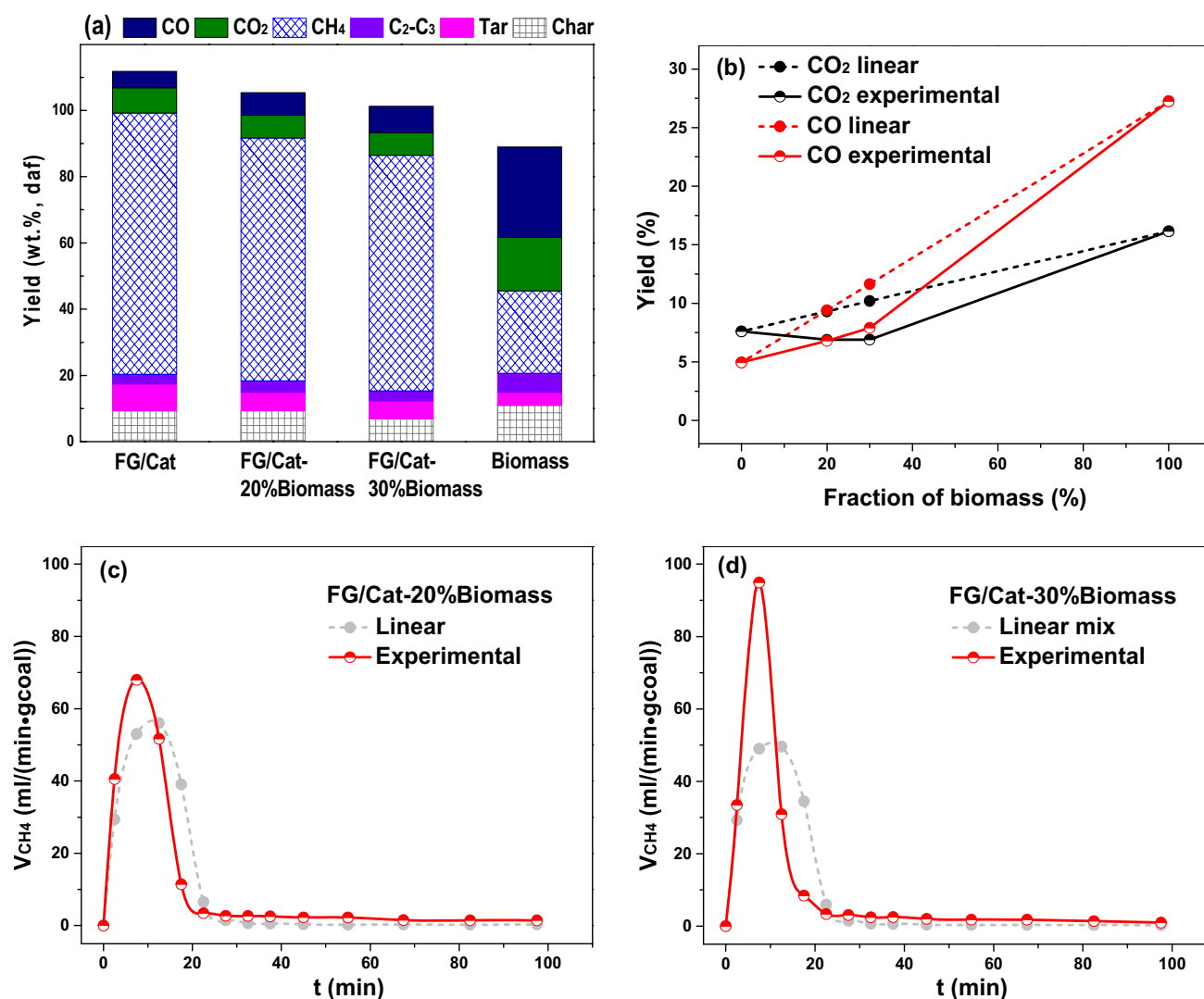


Fig. 22 Experimental results for co-CCHG of FG bituminous coal and biomass (corn stalks, CS) in a fluidized bed (reaction condition: 850 °C, 3 MPa H₂) **a** Product distribution **b** The calculated and exper-

imental yields of CO and CO₂ with blending different fraction of biomass **c** CH₄ formation rate with adding 20% biomass **d** CH₄ formation rate with adding 30% biomass

by 2060 (Xie 2021), respectively. It is worth mentioning that in CO₂ utilization, a hydrogen-rich condition is needed, and expensive supported catalysts with the configuration of complicated physicochemical structures are required (Saeidi et al. 2021). In addition, restricted by the thermal equilibrium of CO₂ methanation, the reaction temperature should not surpass 350 °C to achieve a considerable yield of CH₄, which results in a low kinetic process and low CO₂ utilization capacity (generally less than 5.9 L_{CO₂}/h g_{cat}) (Lee et al. 2021; Shao et al. 2021).

To promote CO₂ utilization efficiency economically, attaining a high conversion rate of CO₂ in a short gas residence time with the use of recyclable and non-noble metals is desired. To this end, developing a coupled process

combining CO₂ catalytic hydrogenation and coal catalytic hydrogasification in one fluidized bed reactor could be a solution. Wherein, the hydrogen-rich atmosphere endows CO₂ hydrogenation, the relatively high temperature and pressure accelerate the CO₂ conversion rate, and the impregnated Fe/Co/Ni-Ca not only acts as the catalyst for coal hydrogasification, but might also promote CO₂ hydrogenation and methanation as the in-situ generated catalyst containing char is rich in mesopore structures and active sites. If this integrated process simultaneously realized a high conversion of coal and CO₂ in one pressurized fluidized bed under the same reaction condition, the CH₄ yield and H₂ utilization efficiency could be boosted greatly, along with the reduced capital investment, operation cost, and energy consumption.

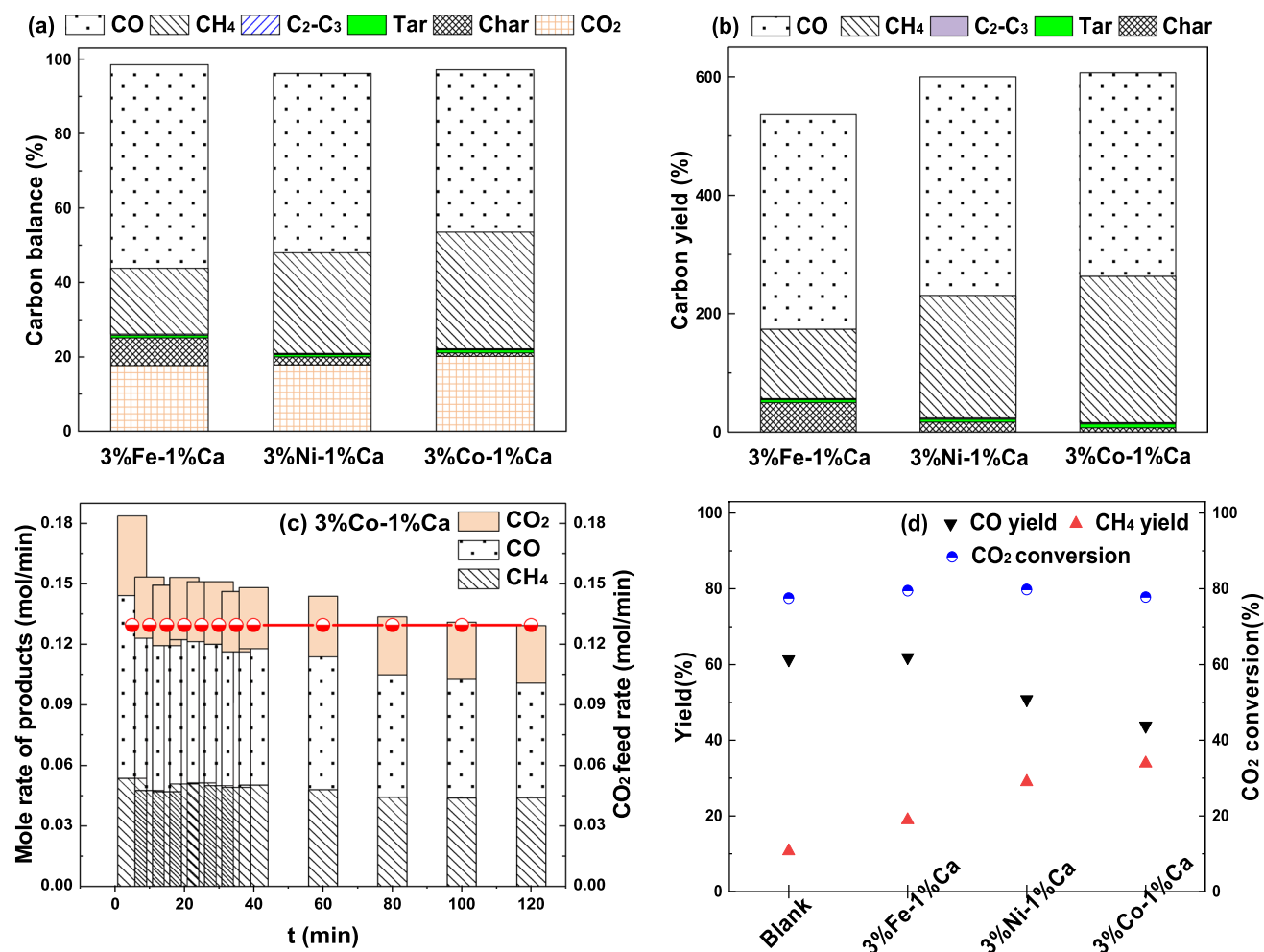


Fig. 23 Co-catalytic hydrogenation characteristics of FG bituminous coal and CO₂ in a pressurized fluidized bed (reaction condition: Fe/Co/Ni–Ca catalyst, 850 °C, 3 MPa, 80%H₂–20%CO₂ with H₂ flow rate 12 L(STP)/min and CO₂ flow rate 3 L(STP)/min) **a** Carbon bal-

ance of the reaction system **b** Product yields on the basis of carbon in coal **c** Main gaseous product formation behavior **d** The yield of CO and CH₄ from CO₂ catalytic hydrogenation ('Blank' refers to CO₂ hydrogenation without the existence of catalyst)

Our group has conducted a pioneering study to integrate coal catalytic hydrogasification and CO₂ catalytic hydrogenation in a fluidized bed (Additional file 1: Methodology S2). Part of the updated data is presented in Fig. 23. It can be seen that CH₄ and CO are the main products with coupling CCHG and CO₂ hydrogenation (Fig. 23a). The catalyst evaluation results demonstrated that Co–Ca catalyst exerts superior activity from the aspects of carbon conversion of coal (92.4%) and CH₄ yield (247%, calculated based on carbon in coal). Remarkably, the CH₄ yield is much higher than that of CCHG in pure H₂ (77.3% in Table 6), suggesting that in the CCHG-to-SNG process, coal resource can be partly substituted by CO₂, because CO₂ catalytic methanation contributes to a high share of CH₄ (more than 50%) when it is coupled with coal catalytic hydrogasification.

Figure 23c shows that Co–Ca catalyzed hydrogenation of coal and CO₂ proceeds to a steady state at 60–80 min,

wherein carbon conversion of coal reaches 92.4%, and CO₂ is the only carbon resource converted to CO and CH₄ with the Co–Ca containing char residue acting as the catalyst. Detailed results in Fig. 23d reveal that Co–Ca containing char possesses profound activity towards CO₂ methanation with CO₂ conversion and CH₄ yield respectively achieved to be 77.8% and 34.5%, which approaches the equilibrium results (79.2% for CO₂ conversion and 36.2% for CH₄ yield). Therefore, although a high temperature is adverse to the methanation of CO₂, the CO₂ conversion rate can be greatly accelerated, making the required residence time for achieving a considerable CO₂ conversion well coupled with the short gas residence time of ~4 s for CCHG in a pressurized fluidized bed. Especially in the presence of Co–Ca containing char as the superior catalyst, the methanation of CO₂ reaches equilibrium in the gaseous residence time of ~4 s, ensuring that large quantities of CO₂ can be dealt with to

generate SNG when CO₂ catalytic hydrogenation is integrated with coal catalytic hydrogasification in a pressurized fluidized bed. According to the preliminary experimental results, it can be calculated that the CO₂ utilization capacity is 17.7 L_{CO₂}/h g_{cat}, while the CO₂-based CH₄ space-time yield is 7.6 L_{CH₄}/h g_{cat}, far surpassing the reported results for catalysis of CO₂ methanation as summarized in Additional file 1: Table S1.

Herein, it is noteworthy that the capacity of dealing 17.7 L_{CO₂}/h g_{cat} is subversive in the progress of CCHG when considering scaling up. As estimated in Sect. 4.5, 5400 t/d coal can be progressed to produce 2 billion cubic SNG/year, wherein 8.7% char residue acts as the catalyst for CO₂ hydrogenation. On this basis, it is calculated that ~5.5 million tons of CO₂ can be dealt with, amounting to 0.015% and 0.048% of the total CO₂ emission in 2022 of the world and China, respectively. This result is striking because approximately 8.8% of CO₂ can be neutralized in China by applying the technology of CCHG to produce 366 billion cubic SNG/year (SNG consumption in 2022). Therefore, the coupling of coal catalytic hydrogasification and CO₂ catalytic hydrogenation in a pressurized fluidized bed provided a novel strategy for SNG production in the context of green manufacturing. Further researches are deserved to investigate the detailed mechanism of catalyst-containing char on CO₂ methanation under CCHG conditions, and also, the acting behavior of CO₂ hydrogenation on coal catalytic hydrogasification can be explored. A clear elaboration of these issues will provide

theory guidance for designing reaction conditions and tailoring product distribution in a practical continuous-fed fluidized bed.

Table 9 summarizes the existing approaches for manufacturing CH₄ from CH₄ production, H₂ consumption, and CO₂ emission perspectives. The detailed calculation procedures for the data and stoichiometric reactions are given in Additional file 1: Methodology S1 and Table S3 of support information, respectively. The results show that CCHG, Co-CCHG of coal and Biomass, and Co-CCHG of coal and CO₂ are emerging approaches for boosting CH₄ production with fewer coal consumptions and CO₂ emissions, which shows advantages over mature TSG and CCG technologies. Herein, it is interesting to find that biomass hydrogasification is a carbon-sinking process with CH₄ as the end of the carbon trajectory; whereas, CH₄ production from CS hydrogasification is unsatisfied. Therefore, the coupling of CS hydrogasification and CCHG might be preferred because the penetration of biomass not only generates additional CH₄, but also mitigates CO₂ emission. Herein, it should be noted that the calculations in Table 9 are based on the supply of 'grey' H₂ (generated from coal gasification), which releases large quantities of CO₂ (11 kg CO₂/kg H₂). Once the 'green' H₂-based technologies from biomass pyrolysis/gasification or wind/solar-induced water electrolysis were matured, CO₂ emissions would be decreased drastically, especially for Co-CCHG of coal and CO₂ and CO₂ catalytic methanation technologies.

Table 9 Evaluation of the production capacity, H₂ consumption, and CO₂ emissions for CH₄ production

Technology ^a	CH ₄ production (Nm ³ /kg coal ^b)	H ₂ consumption ^c (mol/mol CH ₄)	CO ₂ emission ^f (g/mol CH ₄)
TSG	0.32	–	72.64
CCG	0.52	–	44.84
CHG	0.55	1.50	36.00
CCHG	1.07	1.67	38.25
Co-CCHG of coal and biomass ^g	1.38	1.67	26.37
Co-CCHG of coal and CO ₂ ^h	3.5	4.85	12.75
Biomass hydrogasification	0.31 ^c	0.99	–83.66
CO ₂ catalytic methanation ^h	0.17 ^d	5.32	15.10

^aTSG, CCG, and CHG data are adopted from Table 1; FG coal in Table 6 is used for CCHG calculations; Corn stalks in Fig. 22 is used for biomass hydrogasification calculations, and its proximate and ultimate results are given in Table S2;

^bDry basis;

^cThe unit herein is Nm³/kg Biomass;

^dThe unit herein is Nm³/kg CO₂;

^eH₂ consumption was calculated from the stoichiometric reactions in Methodology S1;

^fCO₂ emission was calculated from the stoichiometric reactions in Methodology S1;

^gThe blending amount of biomass is 30 wt%;

^hThe H₂: CO₂ molar ratio is 4:1

6 Conclusions and outlooks

Among the existing coal-to-SNG technologies, coal catalytic hydrogasification seems promising due to a high CH₄ yield, high thermal efficiency, and low emissions. In addition to CH₄, other gas–liquid–char products such as ammonia, HCL, and activated carbon can also be resourced as valuable chemicals and materials. In the past decade, pioneer researches have well performed with a focus on the design of catalyst, the catalysis process of model carbon/coal hydrogasification, and the effect of experimental variables. This paper reviews the above topics systemically, and the critical issues concerning process analysis, opportunities, and strategic approaches for CCHG under the constraint of carbon neutrality are also discussed preliminarily. The main conclusions and future directions are as follows:

- (1) The binary catalysts composed of 1%–5% Fe/Co/Ni and 1%Ca show profound activity toward model carbon/coal hydrogasification. The iron group metals supply active hydrogen (H \cdot) and impair C–C bonds for coal–H₂ reaction, while the calcium compounds promote Fe/Co/Ni distribution, retard Fe/Co/Ni poisoning, and mediate Fe/Co/Ni–C interaction to initiate the Cat–DH effect during pyrolysis and catalytic hydrogenation of graphite carbon (rate determining step) during gasification. The prior findings are meaningful for understanding the macro reaction characteristics, but remain kind of superficial. Comprehensive insights about the active center and the detailed interaction between CaO and Fe/Co/Ni–C structure during hydro-pyrolysis and hydrogasification are paramount for catalyst design and product tailoring. Accordingly, the in-situ characterization techniques (XRD, TEM, X-ray absorption) and DFT calculations should be employed to reveal the catalysis process on a molecule scale.
- (2) The elevation of temperature and H₂ pressure under 600–900 °C and 0.1–8 MPa generally promotes coal conversion and CH₄ yield, wherein CCHG is dynamically controlled. CCHG can be suited to coals with high ash content/caking propensity/high rank/sulfur content properties. The findings provide strategies for mediating the reaction process, such as step-wise hydrogenation to boost CH₄ and HCL yield simultaneously, blending low-rank coals to suppress agglomeration and promote overall reactivity, and mechanically mixing CaO/CaCO₃ to fix H₂S and accelerate CH₄ formation. A universal instinct reaction kinetics for catalytic hydro-pyrolysis and catalytic hydrogasification of coal with diverse properties should be further established to provide a basis for the precise design of a gasifier.
- (3) The pressurized fluidized bed might be the suitable gasifier for CCHG from the viewpoint of millimeter/micrometer-sized particles (< 5 mm), minute-level particle residence time, and high mass/heat transfer efficiency. In the presence of a superior Co–Ca catalyst, it is estimated that 2 billion cubic SNG /year, along with ~66,000 tons HCL and ~16,478 tons NH₃, can be produced in one gasifier with an inner diameter of 3.6 m and coal capacity of 5400 t/d. In addition, the CCHG process generates CH₄ with a high thermal efficiency of 81.8%, little NO_x or SO_x pollutants, and small CO₂ emission (1.71 kg/Nm³ CH₄), which exhibits a distinguishing advantage over the commercialized Lurgi technology and the demonstrated CHG technology. Further researches should perform CCHG in a kilogram-fed continuous fluidized bed to determine the proper coupling parameters for reaction and fluidization, including N, r, and H/D. In addition, the mathematical model of reaction-transfer-fluidization for CCHG deserves to be established through the approach of CFD, which will be helpful for exploring the scaling-up characteristics of the fluidized bed gasifier.
- (4) There are numerous opportunities and strategic approaches for CCHG. Once the “green” H₂ acts as an intermediate “energy vector” for CH₄, the emission of CO₂ in CCHG greatly reduces to ~0.4 kg CO₂/Nm³ CH₄. In addition, the CCHG of coal can be integrated with biomass hydrogasification or CO₂ hydrogenation, by which CCHG-to-SNG is strengthened, and fossil feedstock is partly substituted by renewable resources. Preliminary trials have proved that the coupled CCHG process is reliable in transforming biomass and CO₂ into valuable fuels and chemicals, which would be helpful to circulate carbon in order to diminish the greenhouse effect. Especially for co-catalytic hydrogenation of coal and CO₂, the CO₂ capacity and CO₂-based CH₄ space–time yield amounts to 17.7 L_{CO₂}/h g_{cat} and 7.6 L_{CH₄}/h g_{cat}, respectively, far surpassing the reported results for catalysis of CO₂ methanation in the literature. As a future work, the interaction mechanism between biomass/CO₂ hydrogenation and CCHG can be elaborated, and conducting a detailed process and economic analyses to establish an optimized configuration of the integrated process.

The outcomes of this paper can lay the theory foundation, provide basic data, and create incentives for further researches about designing efficient catalysts and configuring reaction processes for converting carbonaceous resources such as coal, biomass, CO₂, wastes et al. to

value-added products environmentally and efficiently. The bottleneck problem for commercializing CCHG might be the design of efficient and recyclable catalysts. In terms of the expensive Co-based catalyst, how to recover Co from CCHG completely and cycle Co in CCHG with little activity loss is urgent to be addressed. When considering the in-expensive Fe-based catalyst, developing a modulated process for enhancing Fe activity towards the C–H₂ reaction will be of significance.

Supplementary Information The online version contains supplementary material available at <https://doi.org/10.1007/s40789-024-00677-x>.

Acknowledgements The authors gratefully acknowledge financial support from the National Natural Science Foundation of China (22308170), A Project Supported by Scientific Research Fund of Zhejiang Provincial Education Department (Y202250270), the Key research and development project of Shanxi Province (202102090301029), Scientific Research Incubation Program of Ningbo University of Technology (2022TS12), Scientific Research Project Funded by Ningbo University of Technology (2022KQ04).

Author contributions Shuai Yan: Investigation, Writing-Original Draft; Jun Feng: Methodology, Validation; Shenfu Yuan: Visualization, Writing-Review & Editing; Zihong Xia: Validation, Writing-Review & Editing; Fengshuang Han: Formal analysis; Xuan Qu: Supervision, Project administration, Writing-Review & Editing; Jicheng Bi: Conceptualization.

Availability of data and materials The data that support the findings of this review are available on request from the corresponding author.

Declarations

Conflict of interest The authors declare that they have no known competing financial interests or personal relationships that could have appeared to influence the work reported in this paper.

Open Access This article is licensed under a Creative Commons Attribution 4.0 International License, which permits use, sharing, adaptation, distribution and reproduction in any medium or format, as long as you give appropriate credit to the original author(s) and the source, provide a link to the Creative Commons licence, and indicate if changes were made. The images or other third party material in this article are included in the article's Creative Commons licence, unless indicated otherwise in a credit line to the material. If material is not included in the article's Creative Commons licence and your intended use is not permitted by statutory regulation or exceeds the permitted use, you will need to obtain permission directly from the copyright holder. To view a copy of this licence, visit <http://creativecommons.org/licenses/by/4.0/>.

References

- Anthony D, Howard J (1976) Coal devolatilization and hydrogasification. *AIChE J* 22(4):625–656
- Asami K, Ohtsuka Y (1993) Catalytic behavior of iron in the gasification of coal with hydrogen. *Stud Surf Sci Catal* 77:413–416
- Babu S, Talwalkar A, Shah B (1978) Fluidization correlation for coal gasification materials-minimum fluidization velocity and fluidized bed expansion ratio. *AIChE* 74:176–186
- Baker R, Sherwood R, Derouane E (1982) Further-studies of the nickel-graphite-hydrogen reaction. *J Catal* 75(2):382–395
- Banerjee D, Nagaishi H, Yoshida T (1998) Hydropyrolysis of Alberta coal and petroleum residue using calcium oxide catalyst and toluene additive. *Catal Today* 45:385–391
- Bargiacchi E, Candelaresi D, Valente A, Spazzafumo G, Frigo S (2021) Life cycle assessment of substitute natural gas production from biomass and electrolytic hydrogen. *Int J Hydrog Energy* 46(72):35974–35984
- Calderón L, Chamorro E, Espinal J (2016) Mechanisms for homogeneous and heterogeneous formation of methane during the carbon-hydrogen reaction over zigzag edge sites. *Carbon* 102:390–402
- Calderón L, Chamorro E, Espinal J (2017) Understanding the kinetics of carbon-hydrogen reaction: insights from reaction mechanisms on zigzag edges for homogeneous and heterogeneous formation of methane. *Carbon* 118:597–606
- Canel M, Misirlioğlu Z, Sinağ A (2005) Hydropyrolysis of a Turkish lignite (Tunçbilek) and effect of temperature and pressure on product distribution. *Energy Convers Manag* 46:2185–2197
- Casanova R, Cabrera A, Heinemann H, Somorjai G (1983) Calcium oxide and potassium hydroxide catalysed low temperature methane production from graphite and water comparison of catalytic mechanisms. *Fuel* 62:1138–1144
- Cha W, Baek I, Jang H (2007) Hydrogasification of various carbonaceous sources using pressure change properties. *Korean J Chem Eng* 24(3):532–536
- Chang G, Wu W, Shi P, Ma J, Guo Q (2020) A promising composite bimetallic catalyst for producing CH₄-rich syngas from bitumite one-step gasification. *Energy Convers Manag* 205:112408
- Chanthakett A, Arif M, Khan M, Oo A (2021) Performance assessment of gasification reactors for sustainable management of municipal solid waste. *J Environ Manag* 291:112661
- Chen Z, Dun Q, Shi Y, Lai D, Zhou Y, Gao S et al (2017) High quality syngas production from catalytic coal gasification using disposable Ca(OH)₂ catalyst. *Chem Eng J* 316:842–849
- Chen Z, Wang D, Li C, Yang H, Wang D, Lai D et al (2020) A tandem pyrolysis-upgrading strategy in an integrated reactor to improve the quality of coal tar. *Energy Convers Manag* 220:113065
- Chitester D, Kornosky R, Fan L, Danko J (1984) Characteristics of fluidization at high-pressure. *Chem Eng Sci* 39(2):253–261
- Cypres R, Ghodsi M, Feron D (1984) Influence of added alkaline salts on hydrogenation kinetics of coal. *Thermochim Acta* 81:105–112
- Duan Y, Duan L, Anthony E, Zhao C (2017) Nitrogen and sulfur conversion during pressurized pyrolysis under CO₂ atmosphere in fluidized bed. *Fuel* 189:98–106
- Dziembaj R, Makowski W, Chmielarz L (1996) Synergistic effects in the transition metal catalysed hydrogenation of commercial graphites promoted by Ca(NO₃)₂ and pretreated with O₂ or CO₂. *Carbon* 34:913–916
- Ellis N, Masnadi M, Roberts D, Kochanek M, Ilyushechkin A (2015) Mineral matter interactions during co-pyrolysis of coal and biomass and their impact on intrinsic char co-gasification reactivity. *Chem Eng J* 279:402–408
- Fan J, Gao K, Zhang P, Dang Y, Ding Y, Zhang B (2023) Direct transformation of fossil carbon into chemicals: a review. *J Energy Chem* 77:247–268
- Feng J, Yan S, Zhang R, Gu S, Qu X, Bi J (2022) Characteristics of Co–Ca catalyzed coal hydrogasification in a mixture of H₂ and CO₂ atmosphere. *Fuel* 324:124486
- Feng J, Gu S, Zhang R, Qu X, Bi J (2023a) Effect of steam on cobalt-calcium catalyzed coal hydrogasification. *Fuel Process Technol* 249:107868

- Feng J, Yan S, Zhang R, Gu S, Qu X, Bi J (2023b) Recycling and reuse performance of cobalt catalyst for coal hydrogasification. *Fuel* 335:126939
- Gao R, Dou B, Chang Q, Xu J, Dai Z, Yu G et al (2020) Effect of temperature and hydrogen on product distribution and evolution of char structure during pyrolysis of bituminous coal in a drop tube furnace. *Fuel* 267:117078
- Ghodke P, Sharma A, Jayaseelan A, Gopinath K (2023) Hydrogen-rich syngas production from the lignocellulosic biomass by catalytic gasification: a state of art review on advance technologies, economic challenges, and future prospectus. *Fuel* 342:127800
- Gil S, Smoliński A (2015) Experimental study of hydrogasification of lignite and subbituminous coal chars. *Sci World J* 2015:1–9
- Glenk G, Reichelstein S (2019) Economics of converting renewable power to hydrogen. *Nat Energy* 4(3):216–222
- González J, Ramiro A, Sabio E, Encinar J, González C (2002) Hydrogasification of almond shell chars. Influence of operating variables and kinetic study. *Ind Eng Chem Res* 41(15):3557–3565
- González J, Mondragón F, Espinal J (2013) Effect of calcium on gasification of carbonaceous materials with CO₂: a DFT study. *Fuel* 114:199–205
- Haga T, Nishiyama Y (1983) Promotion of nickel-catalyzed hydrogasification of carbon by alkaline-earth compounds. *J Catal* 81(1):239–246
- Haga T, Nishiyama Y (1987) Promotion of iron-group catalysts by a calcium salt in hydrogasification of carbons at elevated pressures. *Ind Eng Chem Res* 26(6):1202–1206
- Haga T, Nishiyama Y (1989) Promotion of iron-group catalysts by a calcium salt in hydrogasification of coal chars. *Ind Eng Chem Res* 28(6):724–728
- Haga T, Ozaki J, Suzuki K, Nishiyama Y (1992) Role of MgO and CaO Promoters in Ni-catalyzed hydrogenation reactions of CO and carbon. *J Catal* 134(1):107–117
- Han J, Wang X, Yue J, Gao S, Xu G (2014) Catalytic upgrading of coal pyrolysis tar over char-based catalysts. *Fuel Process Technol* 122:98–106
- Han G, Zhang P, Scholzen P, Noh H, Yang M, Kweon D et al (2022) Extreme enhancement of carbon hydrogasification via mechanochemistry. *Angew Chem Int Ed Engl* 61(18):e202117851
- He C, Feng X, Chu K (2013) Process modeling and thermodynamic analysis of Lurgi fixed-bed coal gasifier in an SNG plant. *Appl Energy* 111:742–757
- He Z, Sun Y, Cheng S, Jia Z, Tu R, Wu Y et al (2021) The enhanced rich H₂ from co-gasification of torrefied biomass and low rank coal: the comparison of dry/wet torrefaction, synergetic effect and prediction. *Fuel* 287:119473
- Hüttlinger K (1981) Kinetics of hydrogasification of coke catalysed by Fe, Co and Ni. *Fuel* 60(11):1005–1012
- Hirsch R, Gallagher J, Lessard R, Wesslhoft R (1982) Catalytic coal gasification: an emerging technology. *Science* 215(4529):121–127
- Holstein WL, Boudart M (1981) Hydrogenolysis of carbon and its catalysis by platinum. *J Catal* 72(2):328–337
- Hong B, Wang X, Zhou Z, Yu G (2013) A comparison of the gas-product-release characteristics from coal pyrolysis and hydrogasification. *Energy Technol* 1(8):449–456
- Huttinger K, Krauss W (1981) Catalytic activity of coal minerals in hydrogasification of coal. *Fuel* 60(2):93–102
- Inui T, Ueno K, Funabiki M, Suehiro M, Sezume T, Takega Y (1979) Synergistic effect of composite catalysts on the direct hydrogenation of carbon. *J Chem Soc Farad T* 75:1495–1508
- Ipsakis D, Varvoutis G, Lampropoulos A, Papaefthimiou S, Marnellos GE, Konsolakis M (2021) Techno-economic assessment of industrially-captured CO₂ upgrade to synthetic natural gas by means of renewable hydrogen. *Renew Energy* 179:1884–1896
- Jia Y, Huang J, Wang Y (2004) Effects of calcium oxide on the cracking of coal tar in the freeboard of a fluidized bed. *Energy Fuels* 18:1625–1632
- Jiang J, Liu Q, Liu Z (2016) Superior catalytic effect of calcium oxide on the hydrogasification of char for CH₄. *Fuel* 180:737–742
- Jiang J, Liu Z, Liu Q (2017) Synergetic catalysis of calcium oxide and iron in hydrogasification of char. *Energy Fuel* 31(1):198–204
- Jin Y, Hu S, Zhang Z, Zhu B, Bai D (2022) The path to carbon neutrality in China: a paradigm shift in fossil resource utilization. *Resour Chem Mater* 1:129–135
- Lahijani P, Zainal Z, Mohamed A, Mohammadi M (2013) CO₂ gasification reactivity of biomass char: catalytic influence of alkali, alkaline earth and transition metal salts. *Bioresour Technol* 144:288–295
- Lee WJ, Li C, Prajitno H, Yoo J, Patel J, Yang Y et al (2021) Recent trend in thermal catalytic low temperature CO₂ methanation: a critical review. *Catal Today* 368:2–19
- Li W, Yu Z, Guan G (2021) Catalytic coal gasification for methane production: a review. *Carbon Resour Convers* 4:89–99
- Liang Y, Wang F, Zhang H, Wang J, Li Y, Li G (2016) A ReaxFF molecular dynamics study on the mechanism of organic sulfur transformation in the hydrolysis process of lignite. *Fuel Process Technol* 147:32–40
- Liang L, Gao X, Gao F, Mao L, Zhu B, Li G (2022) Preparation and composition optimization of the composite Ni/carbon-based microwave absorbents from coal hydrogasification semicoke. *J Fuel Chem Technol* 50:896–903
- Linares-Solano A, Hippo EJ, Philip L, Walker J (1985) Catalytic activity of calcium for lignite char gasification in various atmospheres. *Fuel* 65:776–779
- Liu Y, Liu Q, Gu J, Kang D, Zhou F, Zhang W et al (2013) Highly porous graphitic materials prepared by catalytic graphitization. *Carbon* 64:132–140
- Liu X, Xiong B, Huang X, Ding H, Zheng Y, Liu Z et al (2017a) Effect of catalysts on char structural evolution during hydrogasification under high pressure. *Fuel* 188:474–482
- Liu X, Xiong B, Huang X, Li J, Zheng Y, Liu Z et al (2017b) Development of Zhundong subbituminous coal char structure during hydrogasification under high pressure. *Int J Hydrog Energy* 42(8):4935–4942
- Liu Y, Guan Y, Zhang K (2019) Toward understanding the reactivity and catalytic mechanism of coal pyrolysis with metal chloride modification. *J Anal Appl Pyrol* 138:196–202
- Liu F, Yu G, Yu D, Chen S, Han J, Yu X et al (2021) Calcium catalytic behavior during in-situ gasification of different aged coal chars in CO₂ and steam. *Fuel* 287:119803
- Lu Q, Yuan S, Chen X, Xie X et al (2023) The effect of reaction condition on catalytic cracking of wheat straw pyrolysis volatiles over char-based Fe-Ni-Ca catalyst. *Energy* 263:125722
- Martin E, Toomajian M (1992) Effect of oxidation and other treatments on hydrogasification rate of coal char. *Fuel* 71:1055–1061
- Masnadi M, Habibi R, Kopyscinski J, Hill J, Bi X, Lim C et al (2014) Fuel characterization and co-pyrolysis kinetics of biomass and fossil fuels. *Fuel* 117:1204–1214
- Masnadi M, Grace J, Bi X, Lim C, Ellis N (2015) From fossil fuels towards renewables: Inhibitory and catalytic effects on carbon thermochemical conversion during co-gasification of biomass with fossil fuels. *Appl Energy* 140:196–209
- Matsumoto S (1991) Catalyzed hydrogasification of Yallourn char in the presence of supported hydrogenation nickel catalyst. *Energy Fuel* 5(1):60–63
- Matsumoto S, Sakagami S (1993) Catalytic gasification activity of iron enhanced by spilt-over hydrogen. *Stud Surf Sci Catal* 77:409–412
- Matsumoto S, Walker P (1989) Catalysis of the concurrent C–H₂O–H₂ and methanation reactions-Inhibition by sulfur. *Carbon* 27(3):395–402

- McKee DW (1974) Effect of metallic impurities on the gasification of graphite in water vapor and hydrogen. *Carbon* 12(4):453–464
- Midilli A, Kucuk H, Topal M, Akbulut U, Dincer I (2021) A comprehensive review on hydrogen production from coal gasification: challenges and opportunities. *Int J Hydrog Energy* 46(50):25385–25412
- Misrihoğlu Z, Canel M, Sinağ A (2007) Hydrogasification of chars under high pressures. *Energy Convers Manag* 48(1):52–58
- Moulijn J, Kapteijn D (2001) Catalyst deactivation is it predictable? What to do? *Appl Catal A Gen* 212:3–16
- Nishiyama Y (1986) Catalytic behavior of iron and nickel in coal-gasification. *Fuel* 65(10):1404–1409
- Nishiyama Y, Haga T, Tamura O, Sonehara N (1990) A kinetic feature of catalytic gasification of carbons—activation of nickel and iron catalysts during gasification. *Carbon* 28(1):185–191
- Ohtsuka Y, Tamai Y, Tomita A (1987) Iron-catalyzed gasification of brown coal at low-temperatures. *Energy Fuel* 1(1):32–36
- Qu X, Yan S, Yan X, Zhang J, Zheng Q, An Y (2019) Role of cobalt and calcium on coal catalytic hydrogasification in a pressurized fluidized bed. *Fuel* 239:347–356
- Qu X, Wang Q, Yan S, Feng J, Zhang J, Zhang R, Bi J (2022) The behavior of the different catalysts for model carbon hydrogasification. *J Fuel Chem Technol* 50:1–10
- Saeidi S, Najari S, Hessel V, Wilson K, Keil FJ, Concepción P et al (2021) Recent advances in CO₂ hydrogenation to value-added products—current challenges and future directions. *Prog Energy Combust* 85:100905
- Saraceno E, Ruocco C, Palma V (2023) A review of coal and biomass hydrogasification: process layouts, hydrogasifiers, and catalysts. *Catalysts* 13:417
- Shao B, Hu G, Alkebsi K, Ye G, Lin X, Du W et al (2021) Hetero-junction-redox catalysts of Fe_xCo_yMg₁₀CaO for high-temperature CO₂ capture and in situ conversion in the context of green manufacturing. *Energy Environ Sci* 14(4):2291–2301
- Si X, Lu R, Zhao Z, Yang X, Wang F, Jiang H et al (2022) Catalytic production of low-carbon footprint sustainable natural gas. *Nat Commun* 13:258
- Skodras G, Panagiotidou S, Kokorotsikos P, Serafidou M (2016) Potassium catalyzed hydrogasification of low-rank coal for synthetic natural gas production. *Open Chem* 14(1):92–102
- Song X, Ma X, Ning G, Gao J (2017) Pitch-based nitrogen-doped mesoporous carbon for flue gas desulfurization. *Ind Eng Chem Res* 56(16):4743–4749
- Song Y, Li Q, Li F, Wang L, Hu C, Feng J et al (2019) Pathway of biomass-potassium migration in co-gasification of coal and biomass. *Fuel* 239:365–372
- Śpiewak K, Czernski G, Porada S (2021) Effect of K, Na and Ca-based catalysts on the steam gasification reactions of coal. Part I: type and amount of one-component catalysts. *Chem Eng Sci* 229:116024
- Steinberg M (2005) Process for conversion of coal to substitute natural gas (SNG). New York, HCEI-8-05-001r2
- Sun H, Zhang F, Bi J, Qu X, Yan S, Zhang J et al (2019) Study of Cu–Ni–Ca composite catalysts in catalytic hydrogasification of char. *Energy Fuel* 33(10):9661–9670
- Sun H, Wang J, Bi J, Zhang R, Qu X, Zhang J et al (2021) Investigating the Cu-based catalysts for char catalytic hydrogasification and its recovery. *Fuel* 294:120567
- Suuberg E, Peters W, Howard J (1980) Product compositions in rapid hydrolysis of coal. *Fuel* 59:405–412
- Suzuki T, Iwasaki J, Tanka K, Okazaki N, Funaki M, Yamada T (1998) Influence of calcium on the catalytic behavior of nickel in low temperature hydrogasification of wood char. *Fuel* 77(7):763–767
- Takarada T, Onoyama Y, Takayama K, Sakashita T (1997) Hydrolysis of coal in a pressurized powder-particle fluidized bed using several catalysts. *Catal Today* 127–136
- Tamai Y, Watanabe H, Tomita A (1977) Catalytic gasification of carbon with steam, carbon-dioxide and hydrogen. *Carbon* 15(2):103–106
- Tian Y, Li J, Wei W, Zong P, Zhang D, Zhu Y et al (2021) Parametric effect of biomass partial hydrolysis process in a downer reactor to co-produce high-quality tar and syngas. *Bioresour Technol* 320:124401
- Tomeczek J, Gil S (2010) The kinetics of coal chars hydrogasification. *Fuel Process Technol* 91:1564–1568
- Tomita A, Tamai Y (1972) Hydrogenation of carbons catalyzed by transition-metals. *J Catal* 27(2):293–300
- Tomita A, Kimura A, Ohtsuka Y, Tamai Y (1983) Sulfur poisoning in the nickel catalyzed gasification of activated carbon in hydrogen. *Carbon* 21(3):225–229
- Tosti S, Spazzafumo G, Capobianco D, Buceti G, Pozio A, Bartucca S (2016) EU scenarios of renewable coal hydro-gasification for SNG production. *Sustain Energy Technol* 16:43–52
- Valizadeh S, Jang S, Hoon G, Lee J, Loke P, Ali M et al (2022) Biohydrogen production from furniture waste via catalytic gasification in air over Ni-loaded ultra-stable Y-type zeolite. *Chem Eng J* 433:133793
- Wang X, Yao K, Huang X, Chen X, Yu G, Liu H et al (2019) Effect of CaO and biomass ash on catalytic hydrogasification behavior of coal char. *Fuel* 249:103–111
- Wang M, Wan Y, Guo Q, Bai Y, Yu G, Liu Y et al (2021) Brief review on petroleum coke and biomass/coal co-gasification: syngas production, reactivity characteristics, and synergy behavior. *Fuel* 304:121517
- Wang G, Guo Y, Yu J, Liu F, Sun J, Wang X et al (2022) Ni-CaO dual function materials prepared by different synthetic modes for integrated CO₂ capture and conversion. *Chem Eng J* 428:132110
- Wood B, Sancier K (2006) The mechanism of the catalytic gasification of coal char: a critical review. *Catal Rev* 26(2):233–279
- Wu Z, Zhang J, Fan Y, Zhang B, Guo W, Zhang R et al (2021) Synergistic effects from co-pyrolysis of lignocellulosic biomass with low-rank coal: a perspective based on the interaction of organic components. *Fuel* 306:121648
- Xie K (2021) Reviews of clean coal conversion technology in China: Situations & challenges. *Chin J Chem Eng* 35:62–69
- Xia Z, Yan S, Chen C, Qu X, Bi J (2021) Three-dimensional simulation of coal catalytic hydrogasification in a pressurized bubbling fluidized bed. *Energy Convers Manag* 250:114874
- Yan S, Bi J, Qu X (2017) The behavior of catalysts in hydrogasification of sub-bituminous coal in pressured fluidized bed. *Appl Energy* 206:401–412
- Yan S, Zhang J, Yan X, Pan D, Ren H, Qu X (2018) Catalytic coal hydrogasification by cobalt–calcium catalyst in a pressurized fluidized bed: Role of hydrolysis and catalysis process. *J Anal Appl Pyrol* 135:251–259
- Yan S, Qu X, Xia Z, Chen C, Bi J (2021) Catalytic hydrogasification characteristic of coal with diverse properties in a pressurized fluidized bed. *Fuel* 296:120652
- Yan S, Qu X, Xia Z, Chen C, Bi J (2022) Effect of experimental variables on coal catalytic hydrogasification in a pressurized fluidized bed. *Fuel* 307:121761
- Yang S, Qian Y, Liu Y, Wang Y, Yang S (2017) Modeling, simulation, and techno-economic analysis of Lurgi gasification and BGL gasification for coal-to-SNG. *Chem Eng Res Des* 117:355–368
- Yu G, Yu D, Liu F, Han J, Yu X, Wu J et al (2020) Different impacts of magnesium on the catalytic activity of exchangeable calcium in coal gasification with CO₂ and steam. *Fuel* 266:117050
- Yuan S (2020) Research and development of production of substituted natural gas by hydrogasification. *Mod Chem Res* 3:5–14
- Yuan S, Zhou Z, Li J, Wang F (2012) Nitrogen conversion during rapid pyrolysis of coal and petroleum coke in a high-frequency furnace. *Appl Energy* 92:854–859

- Yuan S, Qu X, Zhang R, Bi J (2015) Effect of calcium additive on product yields in hydrogasification of nickel-loaded Chinese subbituminous coal. *Fuel* 147:133–140
- Yuan S, Zhang N, Qu X, Bi J, Cao Q, Wang J (2017a) Promoted catalysis of calcium on the hydrogasification reactivity of iron-loaded subbituminous coal. *Fuel* 200:153–161
- Yuan X, Fan S, Choi S, Kim H, Lee K (2017b) Potassium catalyst recovery process and performance evaluation of the recovered catalyst in the K₂CO₃ - catalyzed steam gasification system. *Appl Energy* 195:850–860
- Yuan S, Bi J, Qu X, Lu Q, Cao Q, Li W et al (2018) Coal hydrogasification: Entrained flow bed design-operation and experimental study of hydrogasification characteristics. *Int J Hydrog Energy* 43(7):3664–3675
- Zhan S, Wang X, Hong B, Yu G, Wang F (2012) Experimental study on catalytic hydrogasification of lignite. *J Fuel Chem Technol* 40(1):8–14
- Zhang J, Wang X, Wang F, Wang J (2014) Investigation of hydrogasification of low-rank coals to produce methane and light aromatics in a fixed-bed reactor. *Fuel Process Technol* 127:124–132
- Zhang J, Zheng N, Wang J (2016) Two-stage hydrogasification of different rank coals with a focus on relationships between yields of products and coal properties or structures. *Appl Energy* 173:438–447
- Zhang X, Wang J, Liu Q, Te G, Ban Y, Wang Y et al (2017) The Effects of sodium and alkalinity on the microcrystalline structure and the steam gasification performance of Shengli lignite. *J Anal Appl Pyrol* 125:227–233
- Zhang F, Sun H, Bi J, Qu X, Yan S, Zhang J et al (2019) The evolution of Fe and Fe-Ca catalysts during char catalytic hydrogasification. *Fuel* 257:116040
- Zhang J, Tang J, Liu L, Wang J (2021) The evolution of catalytically active calcium catalyst during steam gasification of lignite char. *Carbon* 172:162–173
- Zhang Y, Zhu J, Wang X, Liang P, Jiao T, Li X (2023) Mechanism of sulfur migration and conversion in pyrolysis/combustion staged conversion process of high sulfur coal. *J Anal Appl Pyrol* 172:106026
- Zhao D, Liu H, Zhu D, Qin M (2020) Effect of O-containing functional groups produced by preoxidation on Zhundong coal gasification. *Fuel Process Technol* 206:106480
- Zhou X, Yang X, Li J, Zhao J, Song S, Hao Z et al (2020) High-pressure rapid hydrogasification of pinewood for methane production using calcium looping concept. *Energy Convers Manag* 203:112247
- Zhu H, Yu G, Guo Q, Wang X (2017) In situ raman spectroscopy study on catalytic pyrolysis of a bituminous coal. *Energ Fuel* 31(6):5817–5827
- Zoheidi H, Miller D (1987) Role of oxygen-surface groups in catalysis of hydrogasification of carbon-black by potassium carbonate. *Carbon* 25(6):809–819

Publisher's Note Springer Nature remains neutral with regard to jurisdictional claims in published maps and institutional affiliations.